JOINT NORWEGIAN-RUSSIAN EXPERT GROUP
for investigation of Radioactive Contamination in the Northern Areas

INVESTIGATION INTO THE RADIOECOLOGICAL STATUS OF THE SITE OF THE SUNKEN NUCLEAR SUBMARINE K-159 IN THE BARENTS SEA

Results from the 2014 research cruise

Edited by Justin P. Gwynn and Vyacheslav I. Shpinkov

JOINT NORWEGIAN-RUSSIAN EXPERT GROUP
for investigation of Radioactive Contamination in the Northern Areas

INVESTIGATION INTO THE RADIOECOLOGICAL STATUS OF THE SITE OF THE SUNKEN NUCLEAR SUBMARINE K-159 IN THE BARENTS SEA

Results from the 2014 research cruise

Edited by Justin P. Gwynn and Vyacheslav I. Shpinkov

Preface

This report presents the results obtained by the joint Norwegian-Russian research cruise in 2014 to the site of the sunken nuclear submarine K-159 in the Barents Sea. The research cruise was conducted onboard the R.V. “Ivan Petrov” of the Federal Service for Hydrometeorology and Environmental Monitoring (Roshydromet).

The expedition was planned and carried out under the Norwegian-Russian expert group for the investigation of radioactive contamination in the Northern areas. It was funded through the Norwegian Government’s Nuclear Action Plan with allocations from the Norwegian Ministry of Foreign Affairs and administered by the Norwegian Radiation Protection Authority.

This report has been written by a joint Norwegian-Russian working group with the following contributors:

From Norway:

Justin P. Gwynn - Norwegian Radiation Protection Authority (NRPA)

Hilde Elise Heldal - Institute of Marine Research (IMR)

Brit Salbu, Ole Christian Lind, Hans Christian Teien - Norwegian University of Life Sciences (NMBU/CERAD)

From Russia:

Vyacheslav I. Shpinkov - Federal Service for Hydrometeorology and Environmental Monitoring (Roshydromet)

Georgii Artemev - Research and Production Association “Typhoon”

Alexey Kazennov - National Research Centre “Kurchatov Institute”

Additionally, logistics and participation in the research cruise, comments and input to the report have been given by:

Oxana Blinova, Iolanda Osvath - IAEA Environment Laboratories, Monaco.

Vidar Lien, Penny Lee Liebig, Ingrid Sværen - Institute of Marine Research

Irina Kashirtseva, Dmitry Romashin, Andrey Epifanov - Research and Production Association “Typhoon”

Oleg Kiknadze - National Research Centre “Kurchatov Institute”

Roman Kasyanov, Dmitry Bosman, Nikolay Popandopulo - SSC “Yuzhmorgeologiya”, Gelendzhik

Yuri Kharevskiy - Radiation, Chemical and Biological Protection Service of the Northern fleet

The research cruise leaders were Hilde Elise Heldal, Institute of Marine Research (Norway) and Vyacheslav I. Shpinkov, Federal Service for Hydrometeorology and Environmental Monitoring (Roshydromet) (Russia). Analytical results and relevant information were provided by the following institutions:

Norwegian Radiation Protection Authority, Institute of Marine Research, Norwegian University of Life Sciences and Institute for Energy Technology (Norway); Research and Production Association "Typhoon" and National Research Centre "Kurchatov Institute" (Russia); Centro Nacional de Aceleradores (CNA), Sevilla (Spain).

Executive summary

The joint Norwegian-Russian cruise to investigate the radioecological status of the site of the sunken nuclear submarine K-159 in the Barents Sea was organized through the Norwegian-Russian expert group as one aspect of the greater cooperation between Norway and Russia with regard to nuclear safety and radiological environmental assessments. The joint Norwegian-Russian cruise in 2014 followed on from previous joint Norwegian-Russian cruises to dumping sites of radioactive waste and sunken nuclear submarines in the Barents Sea, Kara Sea and Novaya Zemlya fjords in the 1990s, 2001 and in 2012.

In 2014, the nuclear submarine K-159 was observed lying upright at a depth of around 246 m at the entrance to Kola Bay. The inspection of the outer hull showed that a number of hatches are missing, that damage has occurred to areas of the deck and that there is a break in the hull towards the stern of the submarine.

Based on the in situ gamma measurements taken next to the submarine, the observed activity concentrations, activity ratios and atomic ratios in seawater and in sediment samples taken close to and in the area around the submarine, there is no indication of any leakage from the reactor units of K-159 to the marine environment.

Comparison of activity concentrations, activity ratios and atomic ratios of the different radionuclides analysed in seawater and sediment samples with other marine areas from a similar time period suggests that the main sources of radionuclides to the area around K-159 are long-range ocean transport from sources further afield and global fallout. It is clear that there is a need for further work to identify the reasons behind the disparity in analytical results reported by Norway and Russia for Sr-90 in seawater.

Although there is currently no indication of any leakage from the reactor units of K-159 to the marine environment, further monitoring of the situation and status of the submarine is warranted. It is clear that K-159 has suffered further damage to its outer hull when or since it sank in 2003, including a break in the outer hull close to the stern. It was not possible during the joint Norwegian-Russian cruise in 2014 to determine whether the sinking and impact on the seafloor has had any effect on the inner pressure hull of K-159. Monitoring of the marine environment around K-159 should be followed closely, especially in connection with any future plans for the recovery of the submarine.

Table of Contents

1. Introduction

1.1 Norwegian-Russian cooperation

In 1992 a Norwegian-Russian expert group was established to investigate radioactive contamination in the northern areas under the joint Norwegian-Russian Commission for Cooperation in the Environmental Sector. At first headed by the Ministry of Environmental Protection of the Russian Federation and the Norwegian Ministry of Environment, the Norwegian-Russian expert group is currently jointly led by the Federal Service for Hydrometeorology and Environmental Monitoring (Roshydromet) from the Russian side and by the Norwegian Radiation Protection Authority (NRPA) from the Norwegian side. The Norwegian-Russian expert group was formed in the light of new information concerning dumping of radioactive waste in the Barents and Kara Seas by the Former Soviet Union and to develop a joint plan to investigate this issue.

The objectives defined for the expert group were:

- To obtain information on the handling, storage, discharge and dumping of radioactive material in the northern areas.
- To investigate, through field work, the actual levels of radioactive contamination in the open Kara Sea and at the dumping sites.
- To locate dumped nuclear waste and identify if any leakage of radioactive substances has taken place.
- To undertake impact and risk assessments for man and the environment.
- To inform the public of the results of these investigations
- The Norwegian-Russian expert group has enabled greater cooperation between Norway and Russia with regard to nuclear safety and radiological environmental assessments. In recent years, the Norwegian-Russian expert group has made significant strides in a number of target areas including:
- Cooperation with Russian nuclear regulatory authorities on regulations, inspections, licensing and permissions with regard to risk reduction, with a particular focus on Andreeva Bay.
- Risk and consequence assessments for actual and potential sources of radioactive contamination in North West Russia.
- The wider use of consequence assessments as a component of decision based processes by Russian regulatory authorities.
- The removal and safe disposal of 180 high activity radioactive sources (RTGs) from light beacons in North West Russia and 71 similar sources from the Russian coastline in the Baltic Sea.
- Continued cooperation through the Norwegian-Russian environmental monitoring programme to document trends in radioactive contamination in the Barents Sea and the extension of the programme to include terrestrial monitoring.
- Cooperation on the environmental impact of radioactive contamination, including joint fieldwork, in the area surrounding the Russian nuclear facility at Majak and consequence assessments for potential accidents at the facility.
- Joint Norwegian-Russian expedtions to dumping sites of radioactive waste in the Kara Sea and Novaya Zemlya fjords in 1992, 1993 and 1994.
- Investigation of potential radioactive contamination in the environment following the raising of Kursk in 2001.

- The joint Norwegian-Russian expedtions to the Kara Sea and Stepovogo Fjord in 2012 to investigate the status of dumped radioactive waste including the nuclear submarine K-27.
- The joint Norwegian-Russian expediton to the site of the sunken nuclear submarine K-159 in the Barents Sea.

1.2 The nuclear submarine K-159

1.2.1 Operational history of the nuclear submarine K-159

K-159 (Project design no. 627A) was a November class nuclear-powered attack submarine (No 289) of the Soviet Northern Fleet. Constructed at the Severodvinsk "Sevmash" shipyard, K-159 was launched on 6 June 1963. K-159 was constructed with a light outer flood hull and an inner pressure hull that contained 9 compartments. Overall, K-159 was 107.4 m in length, 7.9 m wide and with a total displacement of 4050 tonnes (Sarkisov et al., 2009). K-159 was powered by two VMA 70 MWt pressurised water reactors located in compartment no. 5. On the 2nd of March 1965, K-159 suffered an accident involving radioactive discharges into her steam generators contaminating the entire propulsion plant. K-159 was overhauled between 1967 and 1968, underwent scheduled repairs between 1970 and 1972 when both reactor cores were refueled, followed by further repairs from 1979 through to 1980. During the period 1963 to 1984, K-159 carried out 9 individual campaigns totaling 392 days at sea, including 6 campaigns (253 days) following refueling of the reactors. In 1988, K-159 was withdrawn from active service and re-designated as B-159. Both reactors were shut down on October 25th, 1988 and brought to a nuclear safe condition in accordance with the acting Russian technical regulations and standards related to reactor-decommissioning procedures. The measures taken were aimed at ensuring that the reactor cores would remain subcritical in the event of any external impact, fire, flooding or sinking of the submarine. However, the reactor cores of K-159 were not defueled and the submarine remained afloat at the Yokanga base station (Gremikha) until 2003 (Hosseini et al., 2017).

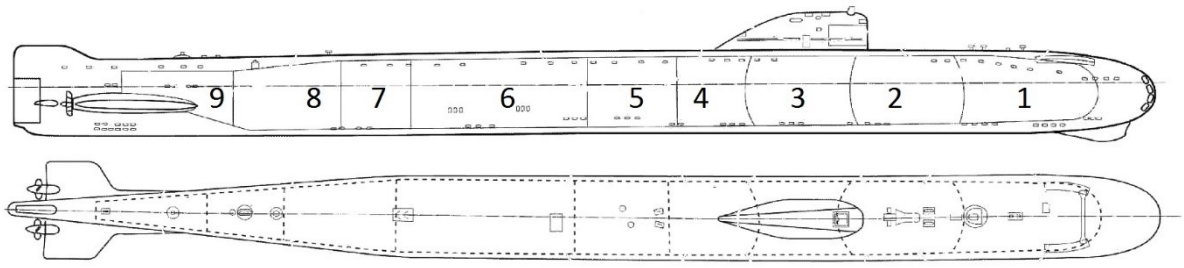

Figure 1.1. Schematic of the nuclear submarine K-159. 1. Torpedo compartment; 2. Sonar and batteries; 3. Control room; 4. Diesel generator and compressor; 5. Reactor compartment; 6. Turbine room; 7. Electric motors and reactor control room; 8. Crew quarters and galley; 9. Steering control.

1.2.2 The sinking of the nuclear submarine K-159

As part of the nuclear submarine decommissioning programme, K-159 was scheduled for transport from Gremikha to the 'Nerpa' shipyard in Snezhnogorsk, Murmansk region for final defueling and dismantling. Prior to transport, a pair of SSP-200 pontoons with a displacement of 200 tonnes were attached to the bow and aft of K-159 to increase the buoyancy of the submarine. The pontoons were attached by ropes to steel plates that had been welded to the outer hull of K-159. K-159 was towed from Gremikha on August 28th, 2003 by a single tug via the bow (Hosseini et al., 2017).

Figure 1.2. The nuclear submarine K-159 under tow from Gremikha with bow and aft pontoons on August 28th, 2003 (Photo: The Russian Northern Fleet).

On August 30th, 2003, the towing tug and K-159 were caught in a storm in the vicinity of Kildin Island with a reported sea state of 4 to 5 and a wind speed of 17 m/s. As a result of the storm conditions, the bow pair of pontoons were torn away from K-159 and seawater flooded compartment no. 8. Subsequently, the aft pair of pontoons were lost and at approximately 3 a.m., K-159 sank to a depth of 246 m at the entrance of Kola Bay (Figure 1.3) at a distance of 6 km from Kildin Island and less than 130 km from the border with Norway (Hosseini et al., 2017). Nine members of the ten towing crew onboard K-159 were lost with the submarine.

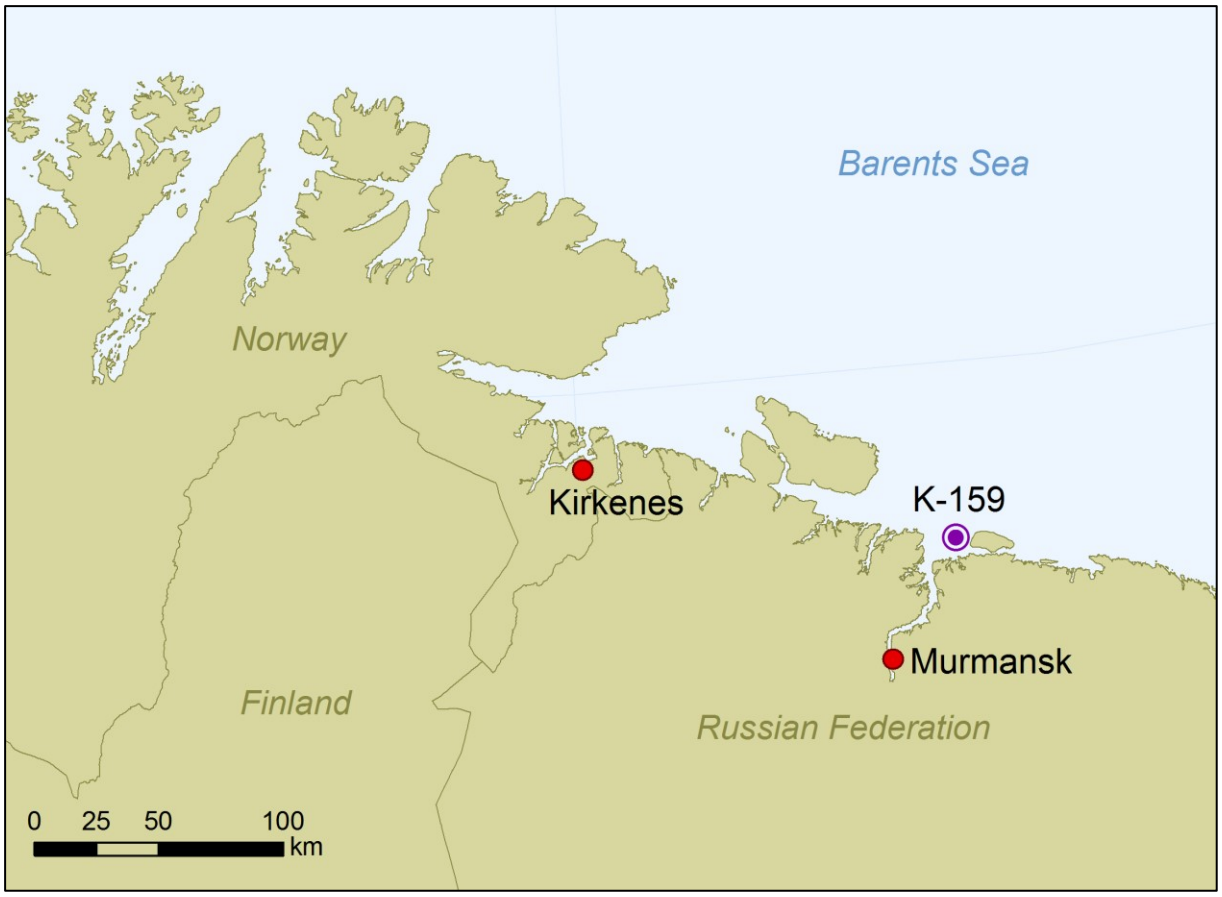

Figure 1.3. The location of the nuclear submarine K-159.

1.2.3 The radioactive inventory of K-159

The total radioactive inventory of K-159 at the time of sinking was estimated by official sources (Minatom) within the Russian Federation at 7.4 PBq (IAEA, 2015). A more recent analysis, using the 'SCALE - 4.3' software code (Rearden and Jessee, 2016) and the known operational history and operating conditions of the reactors in K-159, has estimated that at the time of sinking the total radioactive inventory of K-159 was 3.4 PBq (Hosseini et al., 2017). The spent nuclear fuel (SNF) in the reactors of K-159 is in the form of uranium oxide within an aluminium matrix. The SNF has been estimated to have an enrichment of approximately 20%, corresponding to a total load of 50 to 60 kg of U-235 in both reactors (Hosseini et al., 2017). The sealed primary circuit of each reactor has been reported as containing approximately 5 m^3 of water with specific activities of 1.3 to 1.4 x 10^4 Bq/l in the port reactor and 5.5 to 8.5 x 10^2 Bq/l in the starboard reactor (Hosseini et al., 2017). Taking radioactive decay into account, the estimated inventory of 3.4 PBq would have decreased to 2.6 PBq by September 2014, with greater than 90% of the remaining activity due to Sr-90 and Cs-137 (Hosseini et al., 2017).

1.3 Other potential local sources of radioactive contamination

The Kola Peninsula contains a number of potential sources of radioactive contamination to the marine environment in the area where K-159 lies. The Russian Northern Naval fleet, the mainstay of the Russian Navy, operates nuclear powered surface vessels and submarines from a series of bases in the Kola Peninsula. The Northern Fleet's main base is located at Severomorsk within Kola Bay with additional naval bases at Polyarnyy, Olenya Bay, Gadzhiyevo, Vidyayevo, Bolshaya Lopatka and Gremikha. As well as the presence of military nuclear power vessels, the civilian company Rosatomflot, based just outside of Murmansk, currently operates 6 nuclear-powered icebreakers as well as a nuclear waste treatment plant that discharges directly into Kola Bay. In addition, shipyards that may service military and civilian nuclear powered vessels are located in Murmansk, Roslyakovo, Polyarnyy, Nerpa, and Malaya Lopatka. Previous studies have shown that minor leakages near several military installations in Kola Bay have occurred in the past and that sediments adjacent to the outfall of the Rosatomflot waste treatment plant contained elevated activity concentrations of a number of radionuclides (e.g. Matishov et al., 1999; Brown et al., 2002).

Radioactive waste is handled and stored at a number of locations within the Kola Peninsula. At Saida Bay, a new facility for the processing and long-term storage of radioactive waste has been constructed to receive radioactive waste from naval bases and submarine yards and the civilian icebreaker fleet in the area. Radioactive waste including spent nuclear fuel has been stored at sites of temporary storage at Andreeva Bay and Gremikha. Although the situation at Gremikha is much improved, some 21,000 SNF assemblies and about 12,000 cubic metres of radioactive waste are stored at Andreeva Bay in facilities that have suffered serious deterioration (AMAP, 2010). Failures in containment barriers at Andreeva Bay have led to radioactive contamination of the facility site and the adjacent marine environment at levels above background values for the Barents region (e.g. Sneve et al., 2014; MMBI/ApN, 2015; AMAP, 2016).

1.4 Other regional sources of radioactive contamination

1.4.1 Dumping of nuclear waste in the Barents and Kara Seas

Regular dumping of liquid and solid radioactive waste in the Arctic was practiced by the former USSR and later by Russia from the early 1960s until the early 1990s. Assessments of the total activity of liquid and solid radioactive waste dumped into the Barents and Kara Seas were first reported in the White Book (1993), then revised by the International Arctic Seas Assessment Project (IASAP) in 1993-1996 and subsequently summarised in the IAEA technical document 'Inventory of radioactive waste disposal at sea' (IAEA, 1999). More recently, Sivintsev et al. (2005) reassessed the information originally published in the White Book (1993) and identified a number of errors, inaccuracies and omissions. The total activity of liquid and solid radioactive waste dumped in the Barents and Kara Seas reported by Sivintsev et al. (2005) is 38801.81 TBq, equivalent to approximately 45% of the total activity of radioactive waste dumped in the global oceans (Table 1.1). However it is likely that the true figure is somewhat higher as Sivintsev et al. (2005) identified a number of dumping operations within the Barents and Kara Seas without providing any information on associated activitites of the dumped waste.

Liquid radioactive waste of an activity of 435.2 TBq was deliberately dumped into the Barents Sea within five specially allocated areas, while an additional 522.6 TBq was dumped as a result of

operational accidents in the Barents, Kara and White Seas (Sivintsev et al., 2005). Low- and intermediate-level solid radioactive waste (SRW) was prinicpally dumped in eight main areas covering the fjords east of Novaya Zemlya and the Novaya Zemlya trough in the open Kara Sea. By volume, the bulk of the SRW dumped consists of waste produced during the operation of the naval ships, icebreakers, and submarines with nuclear reactors.

Table 1.1. Total activity (TBq) at time of dumping of different types of radioactive waste dumped in the Arctic region by the Former USSR and Russia as reported by Sivintsev et al. (2005).

Waste type	Total activity at time of dumping (TBq)	Percent of total activity
Reactor units with spent nuclear fuel	21781	56.1
Reactor units without spent nuclear fuel	14802	38.1
Reactor components	20.8	0.1
Low level solid waste	1240.21	3.2
Low level liquid waste	957.8	2.5
Total	38801.81	100

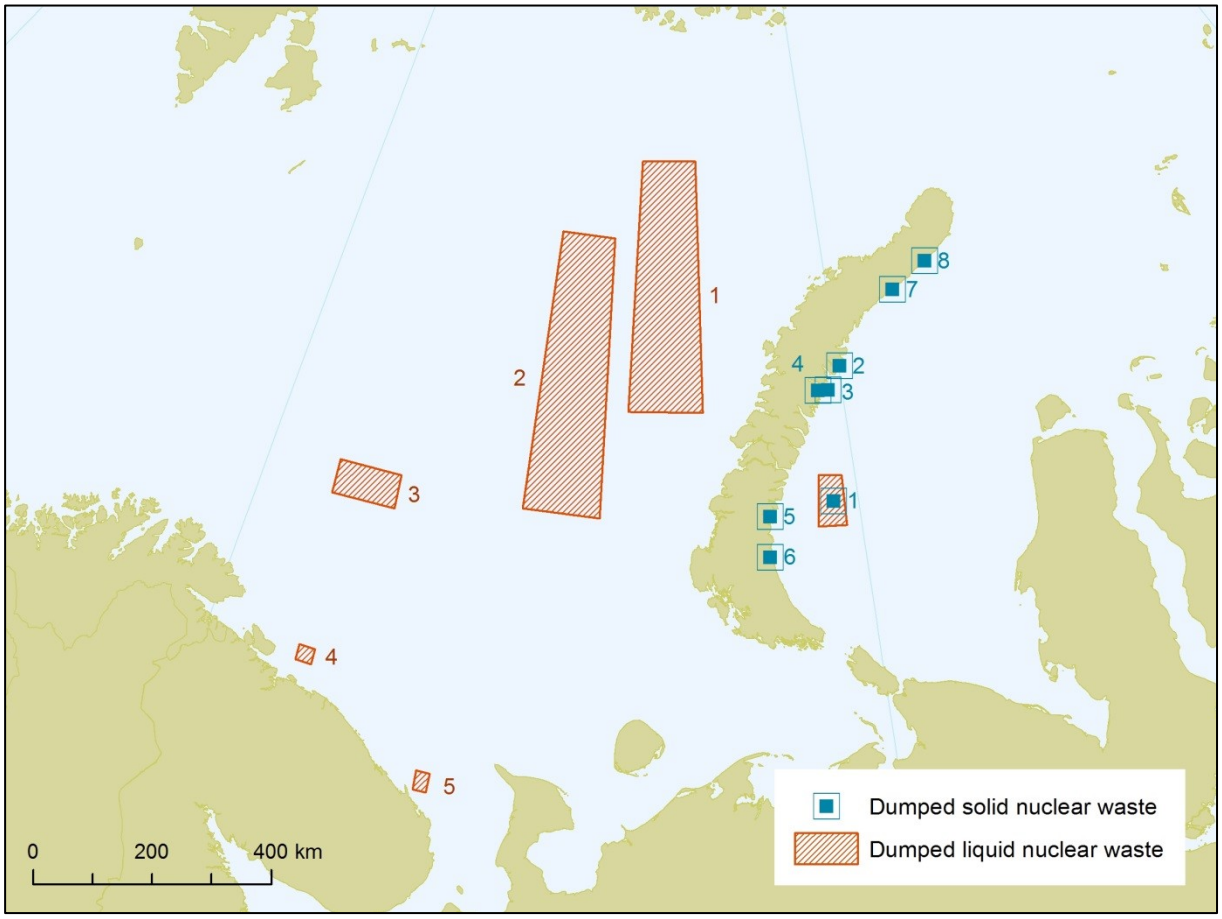

Figure 1.4. Main dumping areas in the Barents and Kara Seas as reported by Sivintsev et al. (2005).

1.4.2 Nuclear weapon testing on Novaya Zemlya

In the period between 1955 to 1990, 130 nuclear weapon tests with a total of 265 megatons were conducted at Novaya Zemlya either in the atmosphere (at high and low altitudes), underground, at sea or underwater. In a regional context (such as Stepovogo Fjord), sources of anthropogenic radionuclides from these tests should be considered as possible contributors to environmental concentrations. Atmospheric tests were mainly carried out over the southern part of the northern island, over both the Barents and Kara Sea coastlines, while 33 of a total of 39 underground tests were carried out at the northern tip of the southern island, approximately 90 km from Stepovogo Fjord. A total of 5 nuclear weapon tests (3 underwater, 1 above water and 1 surface) were carried out in Chernaya Fjord on the south western coastline Novaya Zemlya, while 1 above water test was conducted at Bashmachnaya Fjord further to the west. Subsequent studies in Chernaya Fjord have revealed Pu-239,240 sediment concentrations in excess of 15000 Bq/kg along with elevated levels of Cs-137 and Co-60 (Smith et al., 2000). It has been estimated that approximately 11 TBq of Pu-239,240 is present within sediments in Chernaya Fjord, with evidence from Pu-240/Pu-239 ratios of subsequent transport of this plutonium along the southern coastline of Novaya Zemlya (Smith et al., 2000).

1.4.3 Other sources

In addition to contamination arising from dumped nuclear waste and nuclear weapon testing on Novaya Zemlya, the following sources of radioactive contamination continue to contribute to levels of anthropogenic radioactivity in the Barents and Kara Seas:

- Global fallout from atmospheric nuclear weapon testing in the 1950s and 1960s
- Transport by the rivers Ob and Yenisey of radionuclides originating from global fallout and releases from nuclear installations situated within their catchment areas
- Long range oceanic transport of radionuclides discharged from European reprocessing plants at Sellafield (UK) and Cap la Hague (France)
- Long range oceanic transport of Chernobyl fallout along the Norwegian coast from the Baltic Sea
- The re-entry of the SNAP-9A satellite in 1964

1.5 Previous investigations of the sunken nuclear submarine K-159

1.5.1 Overview of initial investigations

After the sinking of K-159 on August 30th 2003, monitoring of seawater, fish and bottom sediments was carried out the next day by the Service of Radiation, Chemical and Biological Protection of the Northern Fleet with experts from the Kurchatov Institute and IBRAE, RAS. This was followed by further investigations in October and November the same year by the Kurchatov Institute, NIKIET (RDIPE), IBRAE and the Russian Navy to carry out in situ gamma measurements around the outer hull of the submarine. Further investigations were carried out by the Service of Radiation, Chemical and Biological Protection of the Northern Fleet in December 2003 and then in 2004, 2005 and 2007. These studies all concluded that no leakages from the reactors of K-159 to the marine environment had occurred and that observed levels of radioactivity represented background levels only (Sarkisov et al., 2009).

1.5.2 AMEC investigation in 2007

In 2007, further monitoring of K-159 was carried out through international cooperation between the Ministries of Defense of Russia and Great Britain within the framework of the International Programme

for Arctic Military Environmental Cooperation (AMEC). Sampling of seawater and sediments around K-159 were carried out as well as in situ gamma and dose measurements next to and within the outer hull of the submarine, with particular focus on measurements around the reactor section. In addition, high resolution multibeam sonar surveys of the K-159 on the seafloor were performed. The AMEC investigation concluded that no leakages from the reactors of K-159 to the marine environment had occurred. In situ measurements carried out in the spaces between the outer and inner hulls of K-159 indicated that activity concentrations did not exceed 40 Bq/m^3 for Cs-137 and 30 Bq/m^3 for Co-60 (Kazennov, 2010). Activity concentrations of Cs-137 in bottom sediments collected close to K-159 were low (<0.8 to 4.6 Bq/kg d.w.) and did not differ from background values (Hosseini et al., 2017). Based on measurements carried out above the reactor section it was concluded that the spent fuel assembly claddings and the primary circuit were not damaged and it would take a further 30 to 50 years before the spent fuel assemblies might become exposed to seawater due to corrosion (Vasin et al., 2011). However, it was acknowledged that the primary circuit could be compromised sooner which may result in leakages from the reactor section to the marine environment. Results of the high resolution multibeam sonar survey indicated that when K-159 sank it must have struck the seafloor stern first resulting in a break in the outer hull 11.5 m from the aft end of the submarine. K-159 was observed lying up-right on the seafloor with the exception of the last part of the aft section, including the propellers, which was buried vertically in the seabed. It was not possible to assess the condition of the inner hull during the AMEC investigation in 2007.

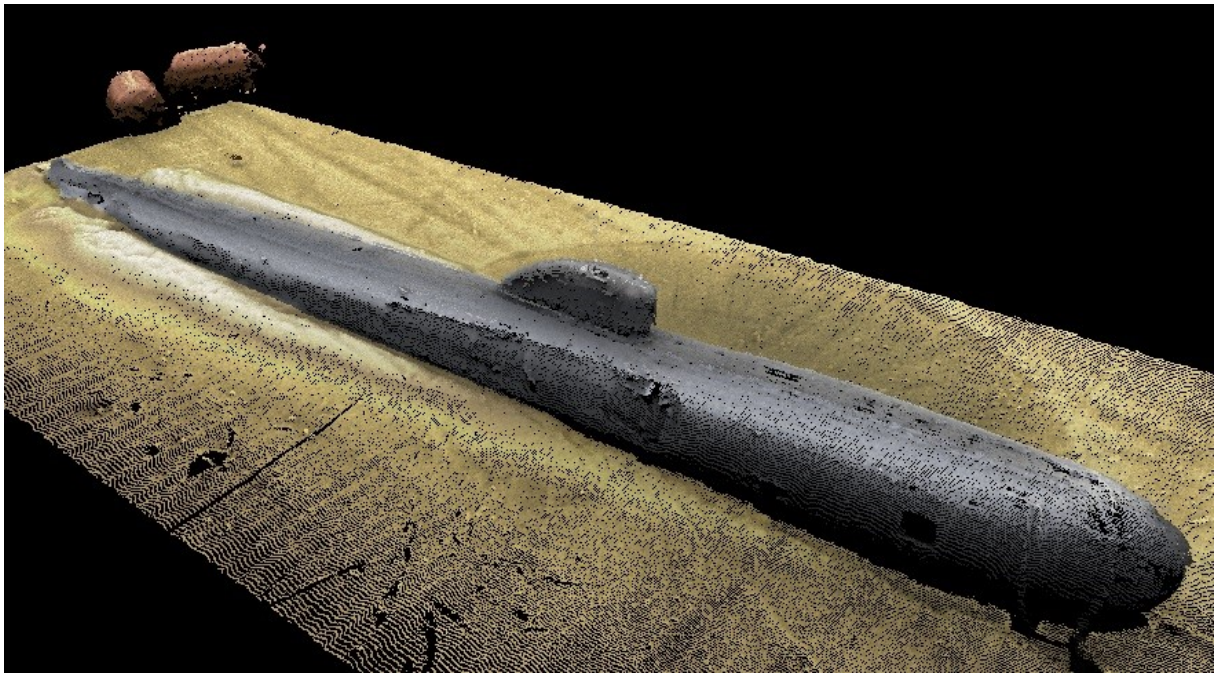

Figure 1.5. High resolution multibeam sonar image of K-159 from AMEC investigation in 2007 (ADUS DeepOcean and Salvage & Marine Operations (S&MO) of the UK MOD).

1.6 The aim of the 2014 Joint Norwegian-Russian Expert Group expedition.

The aim of the 2014 Joint Norwegian-Russian Expert Group expedition was to investigate the radioecological status of the site of the sunken nuclear submarine K-159 in the Barents Sea, through the visual and in situ gamma inspection of K-159 and the collection of environmental samples in the surrounding area.

2. Sampling methodologies

All sampling work was conducted onboard the R.V. “Ivan Petrov” of the Federal Service for Hydrometeorology and Environmental Monitoring (Roshydromet) during September 2014 near the entrance of Kola Bay in the Barents Sea (Figure 2.1). Seawater and sediment samples were collected at a series of sampling stations around and at a distance from the nuclear submarine K-159 close to the entrance of Kola Bay (Figure 2.2).

Figure 2.1. Sailing route to the site of the sunken nuclear submarine K-159 in 2014.

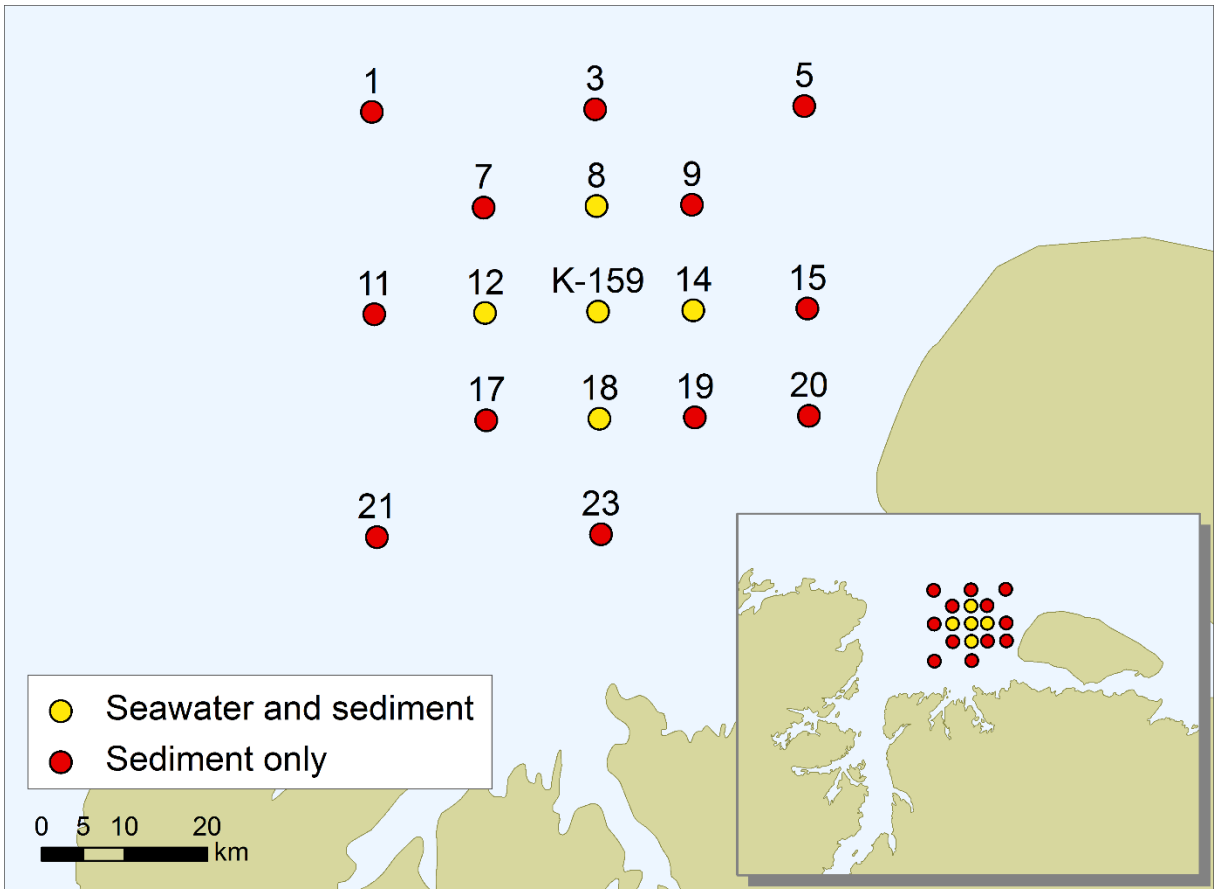

Figure 2.2. Sampling stations in 2014, with relative location of study area inset.

2.1 ROV surveys

Visual and spectrometric inspections of K-159 were carried out with a RT-1000 Remote Operated Vehicle (ROV), equipped with a video camera, a REM-26 NaI gamma spectrometer and a simple sediment collecting device attached underneath the ROV (Figure 2.4a). After K-159 was located with the ROV (Figure 2.4b), a series of in situ gamma measurements were carried out including directly above the reactor compartment, at the stern and next to the conning tower. Count times for in situ gamma measurements were 50 s to ensure a Cs-137 detection limit of approximately 30 Bq/kg in sediments and 1 Bq/l in seawater. Estimates of Cs-137 activity concentrations in sediments by in situ measurements are based on the assumption that all detected Cs-137 occurs in the sediment and through validation of Monte Carlo N-Particle code calibrations. Surface sediment samples were collected using the ROV, by forcing sediment into the collecting device whilst the ROV was driven forward along the bottom. One sediment sample was collected on each of four individual dives at locations around K-159 (Table 2.1). Sediment samples collected by the ROV were first measured onboard and then divided into equal samples for Russia and Norway.

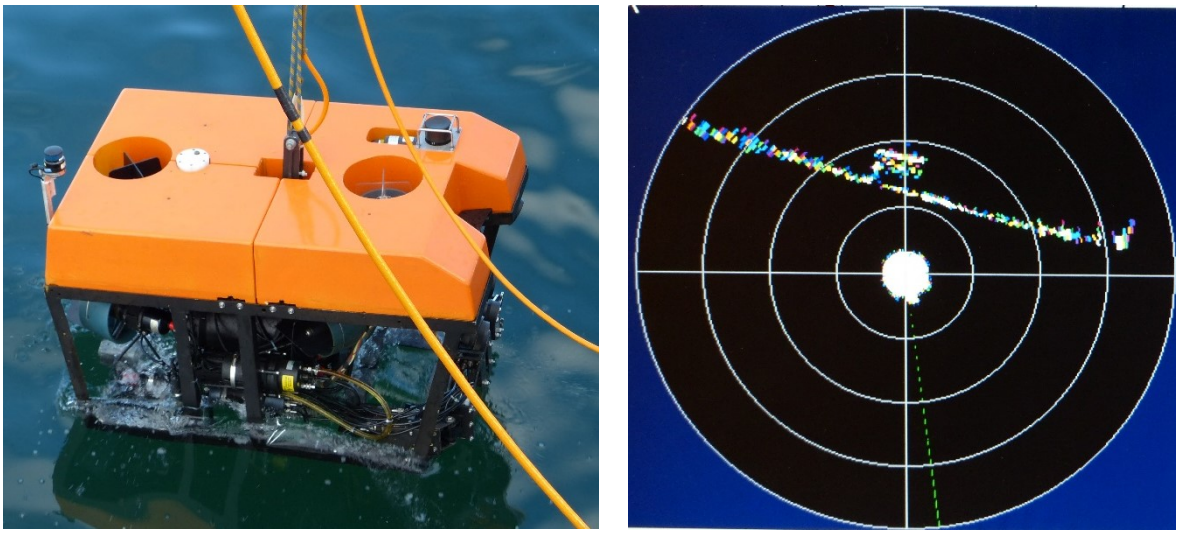

a b

Figure 2.4. a) RT-1000 Remote Operated Vehicle (ROV) and b) K-159 detected on the sonar of the ROV. (Photo NRPA).

Table 2.1. Sediment samples collected with the RT-1000 Remote Operated Vehicle (ROV).

Sample no.	Sampling location around K-159
ROV 1	Near to the bow of the submarine
ROV 2	On the starboard side of the reactor compartment
ROV 3	Near to the stern of the submarine
ROV 4	On the port side of the reactor compartment

2.2 Seawater sampling

Seawater samples were collected at five different sampling stations (Table 2.2). Bottom water samples were collected at all five stations while surface and mid-depth water samples were collected at Station K-159 only (Figure 2.3). Samples collected with a 120 l bottom water sampler (Figure 2.5) were emptied into a large storage tank (220 l) and then divided to ensure that all Norwegian and Russian seawater samples were similar in composition. Surface water was collected separately using submersible pumps while mid-depth water was collected using a 300 l water sampler. Depth profiles of temperature and salinity were recorded at all seawater sampling stations using a SAIV STD/CTD model SD204 attached to the water sampler. Unless stated, all seawater samples were pre-filtered through 1 µm filters before further handling and all seawater samples were stored on deck. Exact sample volumes were determined with the use of flowmeters or graduated cans.

Table 2.2. Overview of seawater sampling by station.

Station ID	Sample type	Depth sampled (m)[1]
K-159	Surface	1
K-159	Mid-depth	100
K-159	Bottom	245
St.8	Bottom	257
St.12	Bottom	265
St.14	Bottom	180
St.18	Bottom	227

1 - Depths for bottom water stations are an average of the maximum depths for each cast from the CTD data.

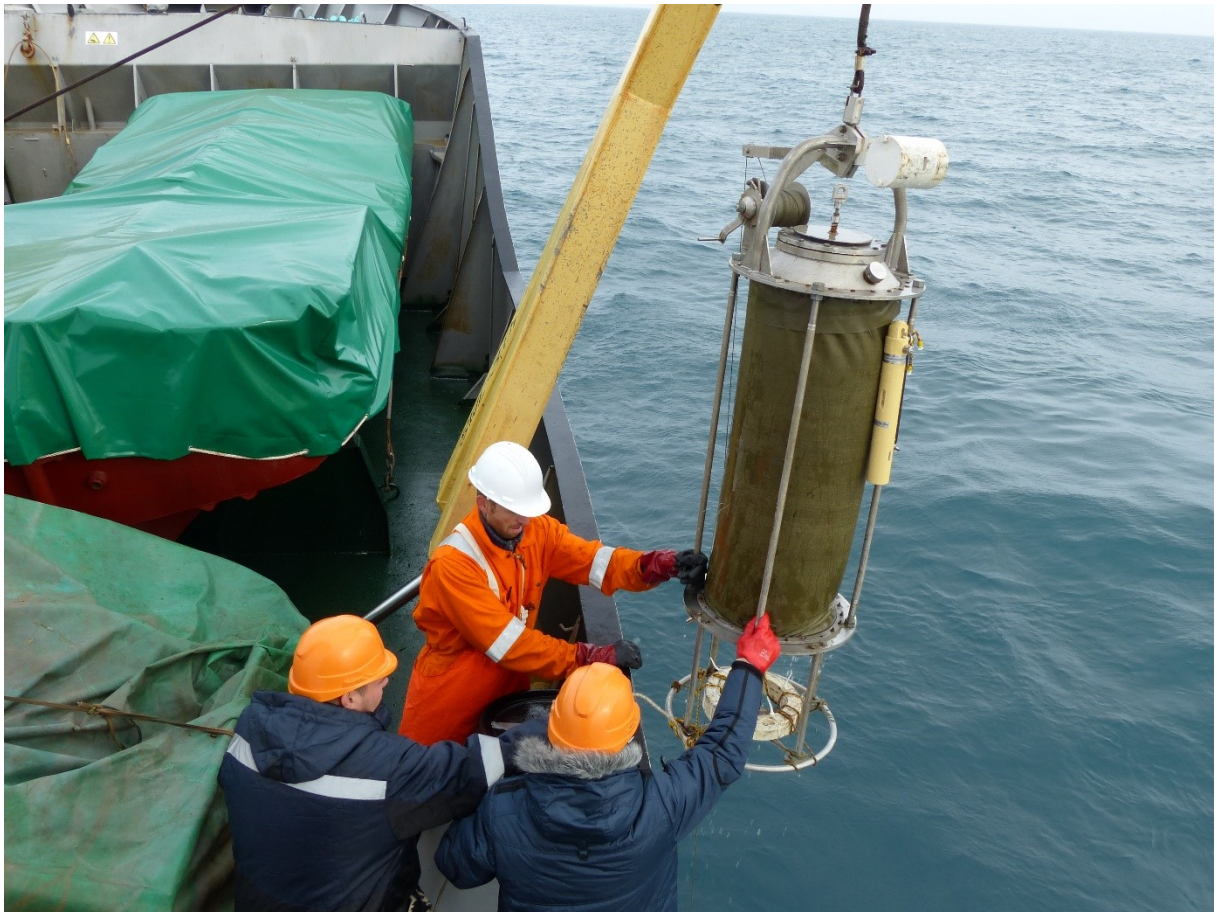

Figure 2.5. Collection of bottom seawater samples with CTD attached to water sampler (Photo NRPA).

2.2.1 Processing of seawater samples onboard by Norway

For Cs-137, a sample volume of around 200 l of pre-filtered seawater was pumped through two 1 µm filters impregnated with cupric hexacyanoferrate at a flow rate of approximately 5 l/min. The filter was then allowed to drip dry, before drying at 60 ˚C.

For Sr-90 (50 l), pre-filtered seawater was collected in 25 l cans and acidified to pH 2 with concentrated HCl. For Pu-239,240 (10 l), pre-filtered seawater was further filtered through 0.45 µm filters and then acidified to pH 2 with concentrated HCl.

In parallel, size and charge fractionation techniques were carried out in order to obtain information on the speciation (physico-chemical forms) of trace metals (e.g. Fe and Cr) and metalloids (e.g. As). Using filtration (0.45 µm Pall filters) and ultrafiltration (Pall hollow fibre cartridge of 10 kDa nominal cut-off) the following fractions were obtained for naturally occurring radionuclides and metals:

- Particles > 0.45 µm
- Pseudocolloids 10 kDa-0.45µm
- Low molecular weight (LMW) forms < 10 kDa

Filtered seawater samples for I-129 (1 l) and trace metal analysis (50 ml) were collected in cans or bottles.

2.2.2 Processing of seawater samples onboard by Russia

For Cs-137, volumes of pre-filtered seawater (200 - 1200 l) were pumped through cartridges containing fibers (Mtilon-T) impregnated with cupric hexacyanoferrate at flow rates up to 500 l/h.

For Pu-239,240, 100 l of pre-filtered seawater was acidified to pH 2 with concentrated HCl, followed by the addition of a Pu-242 yield tracer and 200 g of Na_2SO_3. The sample was stirred periodically for 12 hr prior to the addition of a solution of $FeCl_3$ (1 g Fe^{3+} per 100 l) and then stirred periodically for a further 2-3 hr. A NH_4OH-solution was then added stepwise until the pH of the sample reached 8.5-9. The sample was then left for 12-24 hr to allow the precipitate to settle. The supernatant was carefully removed, to allow collection of the precipitate in a volume of 1.0-1.5 l in a plastic bottle.

For Sr-90, 10 l samples of pre-filtered seawater were collected in plastic bottles and 120 g of Na_2CO_3 was added and stirred for 30 min. After 24-48 hr, the Sr-, Ca-, Mg-carbonate precipitate was then collected by vacuum filtration on a filter. Corresponding pre-filtered seawater samples (250 ml) were collected for determination of stable strontium.

For H-3, 1 l of pre-filtered seawater was collected in a plastic bottle.

2.3 Sediment sampling

Sediment samples were collected using a Smøgen box corer (Figure 2.6a) with an inner area of 30 x 30 cm. At stations 5, 14, 15, 19 and 20, sufficient sediment could only be recovered with the box corer to allow the collection of surface samples. On all other stations, and in addition to surface samples, sediment cores were collected with plastic tubes with an inner diameter of 10 cm. For each station where sediment samples were collected, samples were taken by Russia, Norway and the IAEA.

Sediment cores were cut into 1 cm (0-10 cm) and 2 cm (the remaining core) slices and stored at ambient temperature (Figure 2.6b). Two additional box core samples were taken at station 23. Soft upper sediments from these samples were collected and mixed thoroughly onboard before being divided into 3 samples for intercomparison purposes.

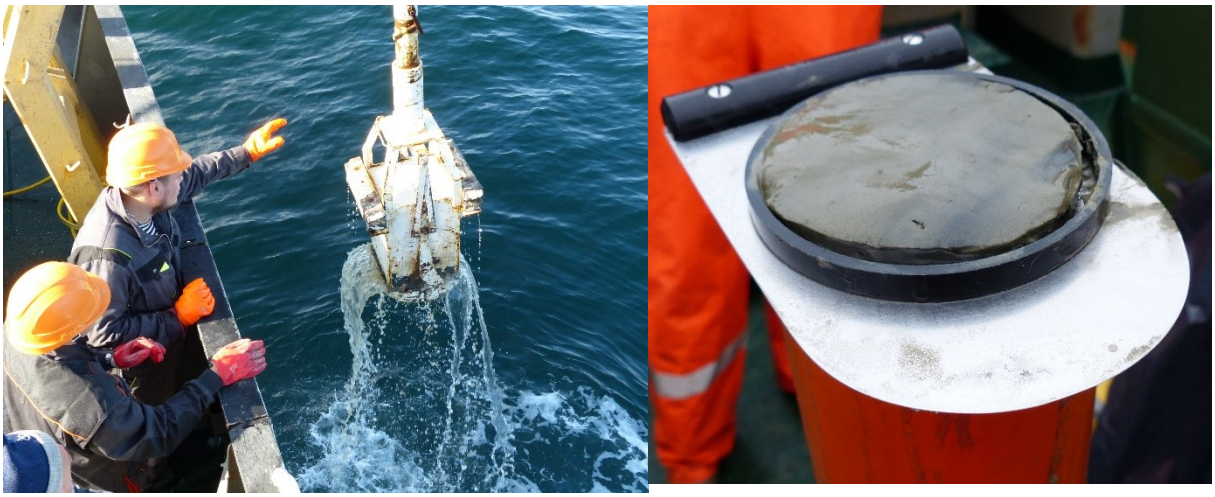

a b

Figure 2.6. a) Retrieval of box corer and b) cutting of sediment core (Photo NRPA).

2.4 Biota sampling

Fish samples were collected at Station 20 using fishing lines (Figure 2.7). Samples of cod (*Gadus morhua*), haddock (*Melanogrammus aeglefinus*) and common dab (*Limanda limanda*) were caught. All fish sampled were measured and weighed before processing. Muscle was sampled from all fish collected, while other tissues (liver, kidney and gills) were sampled from a limited number of each fish species. For samples intended for gamma analysis, muscle samples from each fish of the same species were pooled to provide a bulk sample. For samples intended for trace element analysis all tissue samples (including muscle samples) were treated individually. All samples were dried at 95 ˚C onboard and stored in plastic bags. Where benthic echinoderms (brittle stars) and annelids (polychaete worms) were recovered with the ROV sediments or boxcorer, samples were rinsed in distilled water and dried at 95 ˚C onboard.

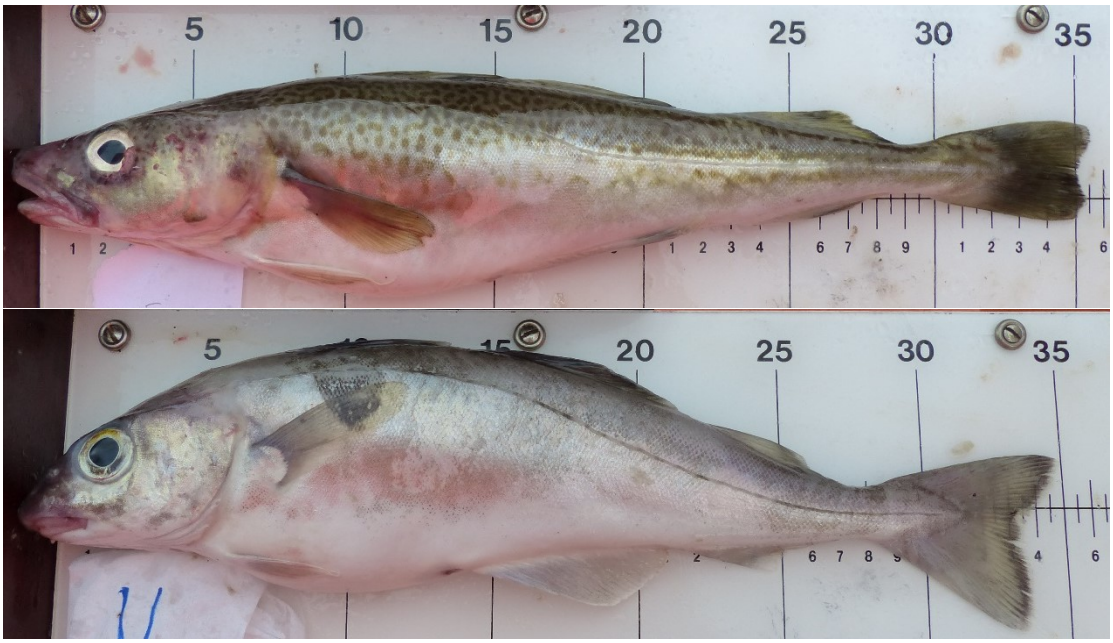

Figure 2.7. Examples of fish samples collected at Station 20 (Photos NRPA). Upper image; cod (Gadus morhua). Lower image; haddock (Melanogrammus aeglefinus).

3. Analytical methodologies

3.1 By Norway

3.1.1 Determination of gamma emitters

In the laboratory, sediment samples were dried at 105 ˚C until constant weight. Cs-137 filters were ashed at 450 °C in a muffle furnace. All sediment samples, Cs-137 filters and biota samples were homogenized before being packed into standard plastic counting geometries and counted on high-resolution gamma spectrometers (HPGe). Spectra were collected for periods of between 1 and 4 days.

3.1.2 Determination of Pu isotopes and Am-241

Pu isotopes and Am-241 were determined from sediment according to the procedure described by IAEA (1989). Briefly, 8-10 g of dried material was ashed overnight at 550 ˚C prior to chemical digestion and separation with Pu-242 and Am-243 added as yield tracers. After chemical separation, plutonium and americium fractions were electrodeposited onto stainless steel discs and their activity determined by alpha spectroscopy on semiconductor silicon detectors.

Pu isotopes and atomic ratios were determined in seawater samples applying a recently published method (Lopez-Lora et al., 2018) using Pu-242 as a yield monitor and TEVA and UTEVA cartridges for Pu isolation and purification. For the determination of Pu atomic ratios in sediment samples, a similar procedure based on the use of ion-chromatographic resins was applied (Chamizo et al., 2008a). Following purification, Pu isotopes and atomic ratios were determined by AMS as described by Chamizo et al. (2008a) and Calvo et al. (2015).

3.1.3 Determination of Sr-90

Sr-90 in seawater was determined according to the standard fuming nitric acid method (Sutton & Kelly, 1968) through its daughter nuclide Y-90, with Sr-85 as a yield tracer. The recovery of the daughter nuclide Y-90 was determined by titration with EDTA according to the method of Varskog et al. (1997), followed by analysis of Y-90 on low background anti-coincidence GM beta counters.

3.1.4 Determination of I-129

I-129 was extracted from seawater samples according to the carrier-free procedure described by Yiou et al. (2004). Briefly, the 1000 ml filtered water samples were acidified with 2 ml of nitric acid and iodine species transformed into I_2 by contact with silver powder (Alfa Aesar Silver Powder Spherical, 635 mesh, 99.9% metal basis) for 24 to 48 hr. The sample was then centrifuged and the supernatant removed. The silver powder was then washed with deionised water (18 MΩ cm) until the pH was neutral and then dried in an oven at 70 °C. Finally, the silver powder was loaded into copper target holders for the measurement by AMS (Chamizo et al., 2008b; Klein et al., 2006; Klein et al., 2007).
I-129 was extracted from sediments based on an alkaline leaching method described by Lopez-Gutierrez et al. (2004). I-129 was then determined by AMS according to the procedure described by Gomez-Guzman et al. (2012).

3.1.5 Determination of trace elements

Trace elements (including U) in all samples were determined in the laboratory by ICP-MS (Agilent ICP-MS 8800 QQQ) from triplicate 50 ml fractionated seawater samples acidified with 5% ultrapure HNO_3 and in gills and livers of fish and in sediments by ultraclave digestion of freeze dried samples with 10% ultrapure HNO_3. The accuracy of the measurements was controlled using the standard reference

materials; CLASS 5, to control seawater measurements; Dolt4, to control measurements of fish (gill and liver) samples; NCS Zc73007, to control measurements of sediments.

3.2 By Russia

3.2.1 Determination of gamma emitters

In the laboratory, sediment samples were dried at 70 ˚C, while Cs-137 filters and fiber sorbents were ashed at 350 °C. All samples were homogenized before being packed into standard plastic counting geometries and counted on high-resolution gamma spectrometers (HPGe). Spectra were collected for periods of between 5 and 32 hr.

3.2.2 Determination of Pu isotopes

Separation of Pu isotopes from precipitated seawater samples was completed in the laboratory by ion-exchange (Procedure, 2004). Pu isotopes in sediment and suspended matter were determined by acid digestion and ion-exchange with Pu-242 as a yield tracer (Procedure, 2004). After chemical separation, plutonium fractions were electrodeposited onto stainless steel discs and their activity determined by alpha spectroscopy on semiconductor silicon detectors.

3.2.3 Determination of Sr-90

Separation of Sr-90 from precipitated seawater samples was completed in the laboratory by co-precipitation (Guidelines, 1986). The yield of the strontium was determined by atomic absorption spectroscopy. Determination of Sr-90 in sediment samples was performed by acid digestion and co-precipitation. The activity of Sr-90 in both cases was determined via Y-90 after ingrowth and separation with a stable yttrium carrier on low background anti-coincidence GM beta counters.

3.2.4 Determination of H-3

H-3 in seawater was determined by distillation and electrolytic enrichment of samples (Methods, 1995), prior to analysis on a low background liquid scintillation beta spectrometer.

3.3 Data handling and quality control

3.3.1 CTD data

Several CTD casts were made at each of the water sampling stations (Stations 8, 12, 14, 18 and K-159). However, most casts were dominated by noise in the conductivity measurements. Therefore, for each station, the casts with least noise were selected for further processing. Spikes and clear instabilities (density decreasing with depth) were removed manually by inspection. To remove additional noise, the vertical profiles were then interpolated to 1 m vertical resolution using bi-linear interpolation and then smoothed using a 5-point (5 m) moving average. Finally, to further reduce signal noise, 2 different casts were averaged to produce profiles at Station 8 and 14. Profiles for Stations 12, 18 and K-159 represent data from individual casts.

3.3.2 Analytical data

Unless otherwise stated, data is reported as individual values with associated uncertainties (2 sigma), as individual mean values of Norwegian and Russian values (where available) for samples taken at the same sampling location with associated standard deviations or as means of individual values with

associated standard deviations. Inventories, activity ratios and atomic ratios based on individual measurements are reported with their propagated uncertainties (2 sigma). Sources of data for individual measurements, mean values, activity ratios and atomic ratios (i.e. Norway or Russia) are indicated in all data tables and figures. Data reported as 'surface sediments' is based on gross surface samples (assumed to represent 0 to 2 cm).

Sediment distribution coefficients (K_d) for radionuclides were derived using data for bottom water and surface sediments from the same station (mean of ROV sediment data for I-129) using activity concentration data from seawater samples filtered through <1 µm (Cs-137) or <0.45 µm (Pu-239,240 and I-129) filters. K_ds for trace elements were derived using mean concentration values for ROV sediments and concentration values from bottom water from Station K-159 filtered through <0.45 µm filters. Bioconcentration factors (BCF) for Cs-137 were derived using the mean Cs-137 activity concentration of all bottom seawater samples filtered through <1 µm filters and the Cs-137 activity concentration data (f.w.) for each pooled fish sample. BCFs for trace elements in fish tissues and other biota were derived using mean concentration values of all bottom seawater samples filtered through <0.45 µm filters.

K_ds were derived by:

K_d = Activity concentration in sediment (Bq/kg d.w.)/Activity concentration in seawater (Bq/l)

BCFs were derived by:

BCF = Activity concentration in biota (Bq/kg f.w.)/Activity concentration in seawater (Bq/l)

Due to problems in exporting sediment samples from Russia, no data for Norwegian sediment samples (other than ROV sediments) or IAEA sediment samples were available at the time of completing this report. During the JNREG expedition in 2012, a sediment sample was taken for intercomparison purposes. The results of the analysis of this intercomparison sediment sample for Cs-137, Sr-90, Pu-239,240 and Am-241 by different laboratories in Norway, Russia and at the IAEA showed good agreement overall (JNREG, 2014). Of the results from the JRNEG expedition in 2014, data reported by Norway and Russia showed good agreement in the case of Cs-137 in seawater and Cs-137 and Pu-239,240 in sediment, but not in the case of Sr-90 in seawater. Norway and Russia reported data for Pu-239,240 in seawater for different size class fractions. The issue of data for Sr-90 in seawater is discussed in more detail in the results chapter (See section 4.3.2). Only Russia reported data for Sr-90 in sediments. Due to the disparity of analytical results for Sr-90 in seawater, sediment distribution coefficients for Sr-90 have not been derived.

4. Results of investigations at the site of the sunken nuclear submarine K-159

4.1 Oceanography

The southern Barents Sea is dominated by relatively fresh water masses (due to river runoff) carried eastward in a coastal current and more saline water masses flowing eastward further offshore derived from the inflow of Atlantic Water. However, as K-159 is located on the eastern slope of the deep at the entrance to Kola Bay, there will be a strong topographic control on the local current pattern.

The vertical profiles of temperature and salinity (Figure 4.1) clearly indicates coastal water in the upper parts of the water column and Atlantic influenced water masses closer to the bottom. However, even near the bottom, there is a substantial influence of coastal water, as the salinity is lower than the 35.0‰ commonly used as a lower bound for Atlantic Water. Furthermore, the profiles show a strong pycnocline in the upper ~20 m. Below 100 m water depth, the stratification is considerably weaker and mostly due to vertical gradients in temperature. While the temperature varies little between the different stations, there seem to be a clear distinction in salinity. Station 8 is the northernmost station and most influenced by the offshore Atlantic Water. However, although station 12 is located in the deepest part outside Kola Bay, it is the station most influenced by coastal water. It is highly likely that mesoscale dynamics such as eddies and meanders, as well as tidal movements influence the local oceanography.

Temperature-salinity plots indicate isopycnal (along lines of constant density) and diapycnal (across lines of constant density) mixing (Figure 4.2). Notably, mixing seems to be occurring between some distinguishable features located at approximately similar depths at Stations 8, 18 and K-159. These observations indicate that turbulent mixing is occurring in the area of investigation.

Based on an analysis of vertical velocity shear between the different stations, a relatively strong, density-driven northward flowing coastal current was identified in the investigated area. Between Stations 12, 14, and K-159, an integrated vertical velocity shear of about 20 cm/s could be observed. Furthermore, using the density difference between Stations 14 and K-159, the magnitude of the vertical velocity shear exceeded the critical value for turbulent mixing at several depths. East of K-159, a more variable flow was identified, with a flow reversal between 100 and 150 m depth. From the investigations in 2007, a near-bottom current, likely induced by tidal currents, of 41 to 62 cm/s was reported (Sarkisov et al., 2009), indicating that the ocean currents in the area are relatively strong and variable.

It was not possible to obtain detailed bathymetric measurements during the cruise, but from the previous high-resolution sonar surveys in 2007, K-159 has been shown to lie on a seafloor that slopes gently downwards from the east and shallower waters adjacent to Kildin Island to the west and deeper waters outside Kola Bay (Figure 4.3). Sarkisov et al. (2009) reported that the seafloor gradient at the location where K-159 lies was approximately 2°.

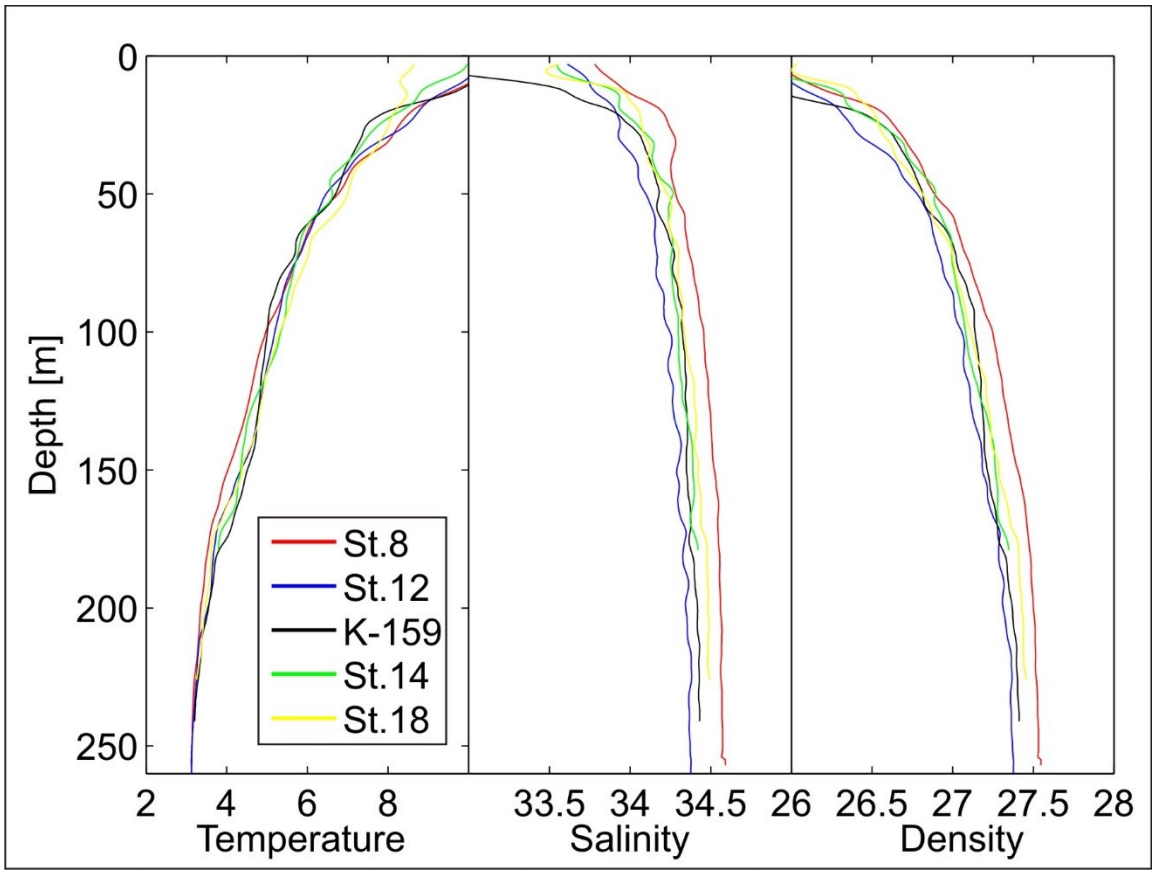

Figure 4.1. Vertical profiles of hydrographic properties for water sampling stations.

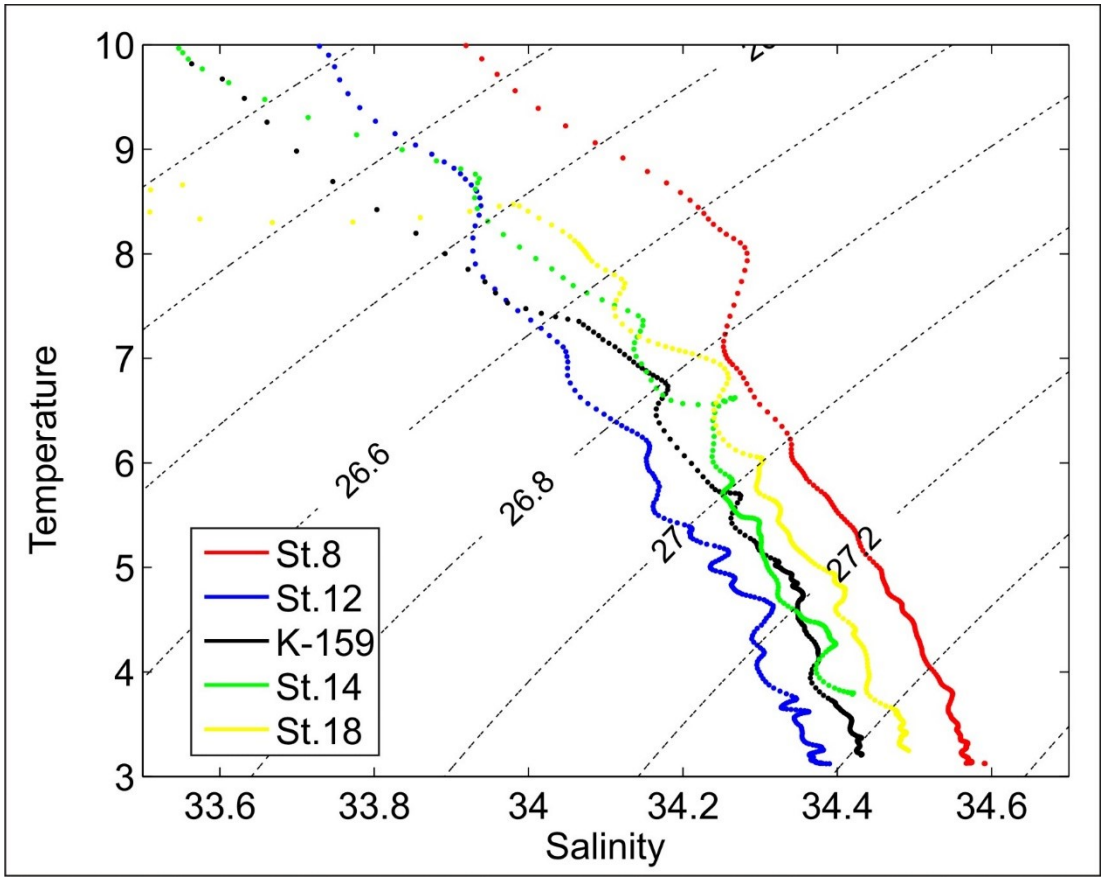

Figure 4.2. Temperature-Salinity plots for water sampling stations.

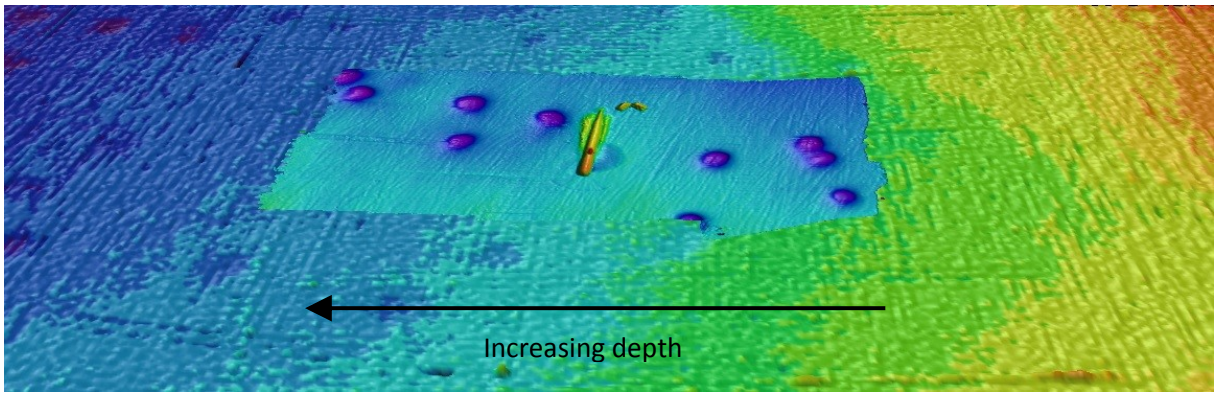

Figure 4.3. False colour side-scan sonar image of the bathymetry of the seafloor in the area around K-159 (ADUS DeepOcean and Salvage & Marine Operations (S&MO) of the UK MOD). Increasing depth from east to west indicated by colour grading from orange to blue. Higher resolution central panel showing location of K-159.

4.2 Visual inspection and in situ gamma measurements

The exact location of the sunken nuclear submarine K-159 was determined by the sonar on the ROV. Video pictures showed that K-159 lies upright on the seabed with the deck of the submarine covered in a layer of sediment. A number of different fish species and other biota were observed around the submarine. The inspection of the outer hull showed a number of missing hatches, some damage to areas of the deck and the break in the hull towards the stern of the submarine that was reported by the AMEC 2007 investigation. By comparison with photos of K-159 as it was being towed out from Gremikha in 2003 (e.g. Figure 1.2), it is clear that the loss of some hatches and the observed damage to the deck and stern must have occurred when or since K-159 sank. It was not possible to visually assess the status of the inner pressure hull of K-159. (Figure 4.4).More than 100 spectra were collected at locations close (1-3 m) to the hull of the sunken nuclear submarine K-159 (Figure 4.5). No Cs-137 or any other artificial radionuclides were detected at levels exceeding the minimum detectable activity of the underwater gamma-spectrometer in any of the in situ measurements recorded for seawater or sediments (Figures 4.6 and 4.7), as was reported by the last investigation of K-159 in 2007 (Kazennov, 2010).

Tower (back view)

Reactor compartment

Fish near bow of submarine

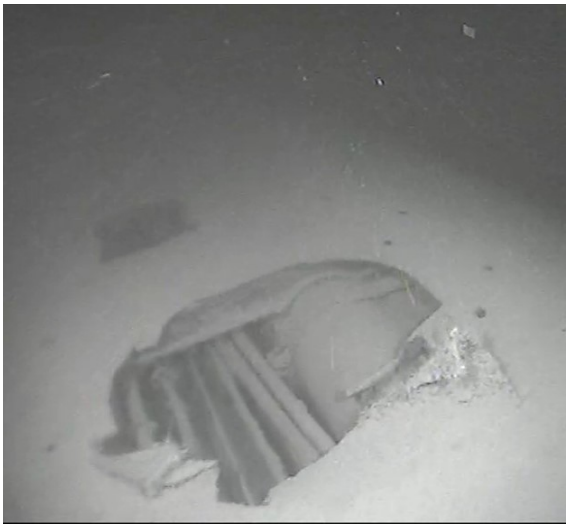

Damage to outer hull

Damage to outer hull close to stern

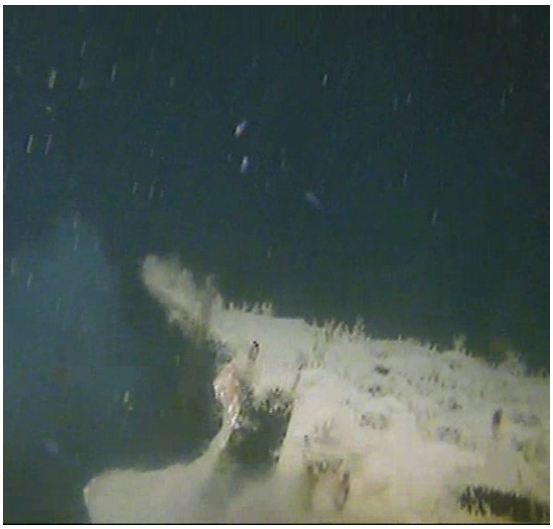

Break in the hull towards the stern of the submarine

Figure 4.4. Images taken from the video surveillance of the sunken nuclear submarine K-159.

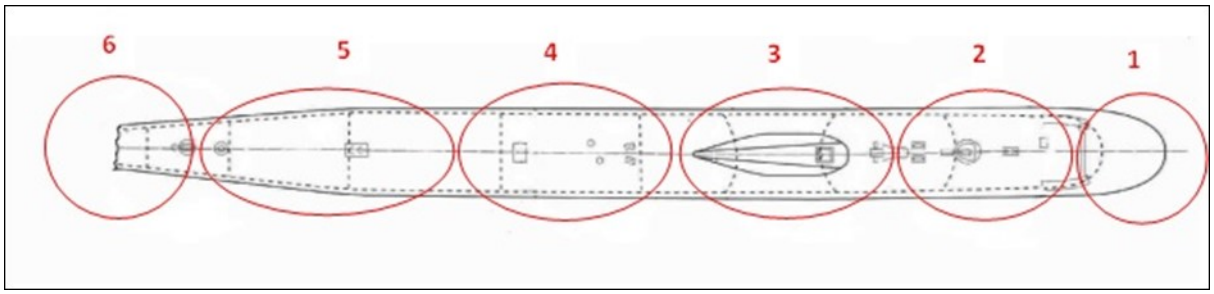

Figure 4.5. Locations where in situ gamma spectra were obtained close to the hull of the sunken nuclear submarine K-159.

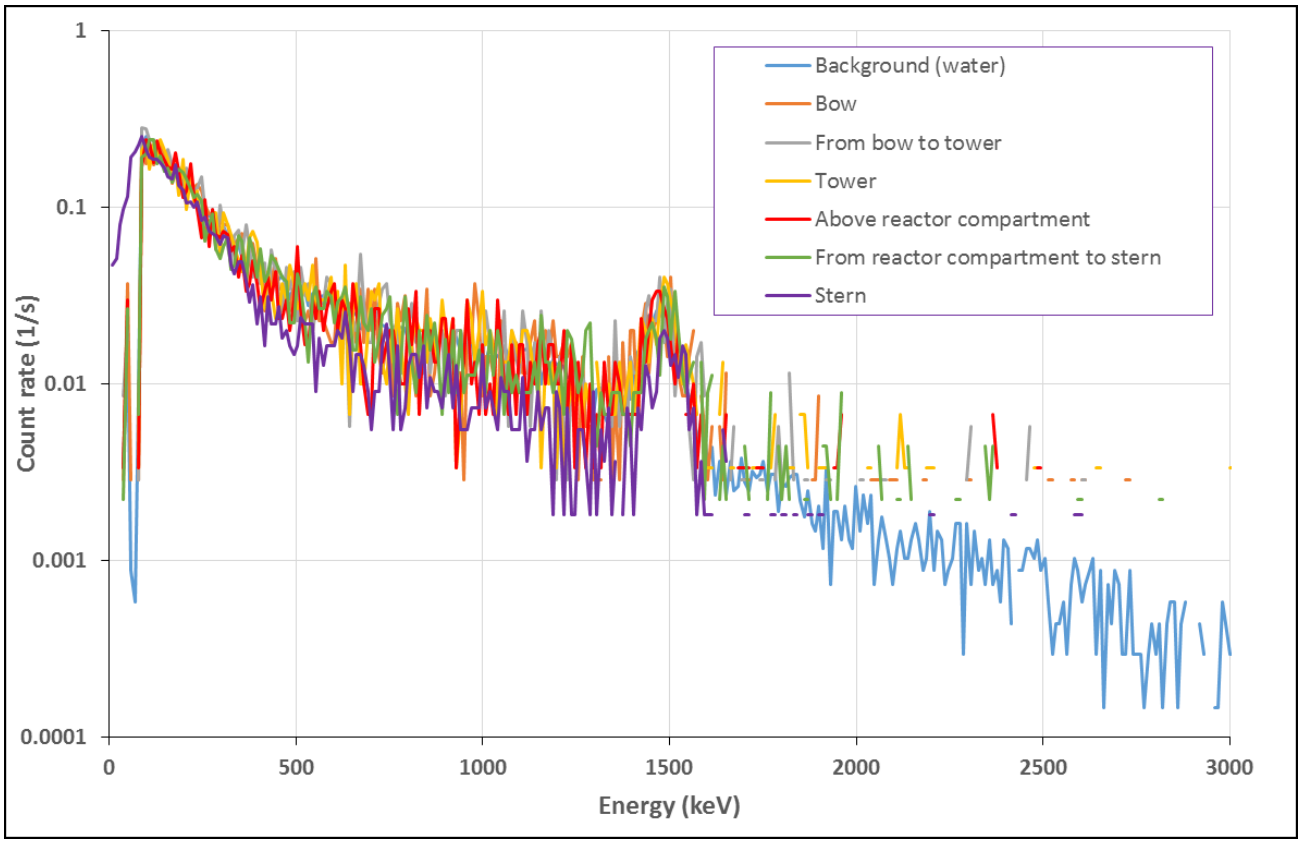

Figure 4.6. In situ gamma spectra for seawater close to the hull of the sunken nuclear submarine K-159.

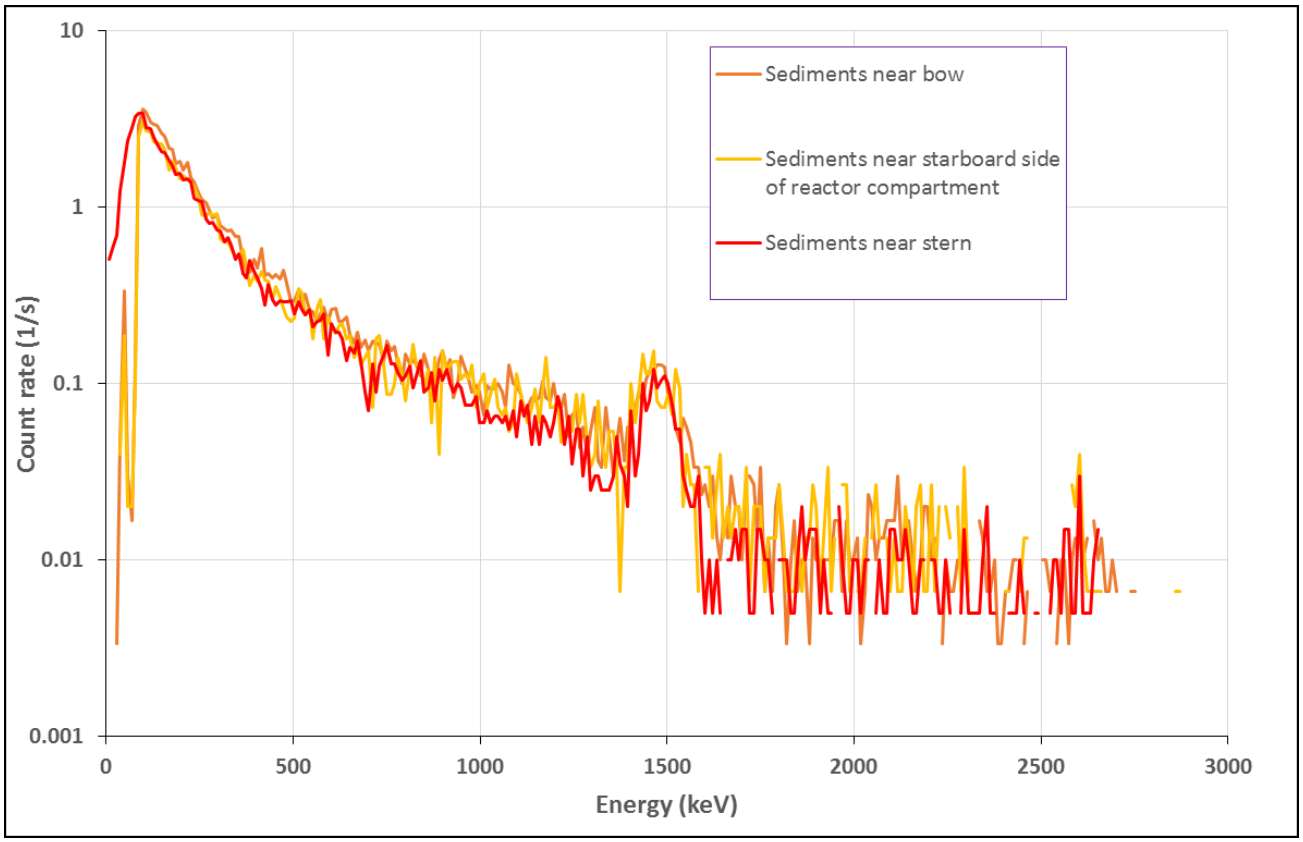

Figure 4.7. In situ gamma spectra for sediment close to the hull of the sunken nuclear submarine K-159. The higher count rates for spectra for sediment compared to seawater are expected due to the combination of the shielding effect of seawater, the proximity of the detector to the seafloor and the typically higher content of naturally occurring radionuclides in sediments.

4.3 Radionuclides and trace elements in seawater

4.3.1 Cs-137

The mean activity concentration of Cs-137 observed in filtered bottom seawater collected near K-159 was 1.7 ±0.1 Bq/m^3 which was similar to values for all other sampling depths and stations at between 1.5 and 2.0 Bq/m^3 (Table 4.1). The Cs-137 activity concentrations in seawater from the sampling area in 2014 were comparable to values previously reported for the southern Barents Sea in 2008 and 2009 (Leppänen et al., 2013) and for the Pechora Sea and Kara Sea in seawater sampled during the JNREG expedition in 2012 (JNREG, 2014).

In comparison with other marine regions in 2014 (Figure 4.8), the Cs-137 activity concentrations in seawater at Station K-159 were similar to reported values for the Barents Sea (Skjerdal et al., 2017), but lower than mean values for the Norwegian Sea and the Kattegat & Skagerrak (Skjerdal et al., 2017), the North Sea (BfS/BMU, 2017), for waters in the Baltic Sea region (HELCOM, 2015) and the Irish Sea (EPA, 2016). This pattern reflects the long-range ocean transport of Cs-137 originating from authorised discharges of this radionuclide from European reprocessing plants at Sellafield (UK) and Cap la Hague (France) as well as fallout from the Chernobyl accident.

With regard to possible fluxes of Cs-137 from local sources, activity concentrations of Cs-137 in seawater of up 5 ±1 Bq/m^3 have been reported recently for seawater from Andreeva Bay (MMBI/ApN,

2015). However, in the same study, coastal water samples taken between Andreeva Bay and Kola Bay showed activity concentrations of Cs-137 (1.0 to 2.1 Bq/m^3) that were similar to values typical for the Barents Sea as was the case for seawater samples (1.0 to 1.4 Bq/m^3) taken within Kola Bay (MMBI/ApN, 2015). Taking all available data together, activity concentrations of Cs-137 in seawater in the area around K-159 in 2014 were typical of values for the region, with the main source of Cs-137 to this area likely to be the long-range ocean transport of Cs-137 from sources further afield.

Table 4.1. Cs-137 and Sr-90 activity concentrations (Bq/m^3) in filtered seawater (<1 µm) from Station K-159 compared to other sampling stations.

Station	Depth	Cs-137 (Bq/m^3)[a]	Sr-90 (Bq/m^3)	
			Norway	Russia
K-159	S	1.5 ±0.1	0.99 ±0.11	2.6 ±0.5
	M	2.0 ±0.2[b]	-	4.3 ±0.6
	B	1.7 ±0.1	0.87 ±0.13	5.0 ±1.0
St.8	B	1.8 ±0.2	0.76 ±0.10	3.7 ±0.7
St.12	B	1.5 ±0.1	1.07 ±0.15	3.2 ±0.6
St.14	B	1.7 ±0.2	1.07 ±0.12	3.7 ±0.7
St.18	B	1.5 ±0.2	0.69 ±0.09	1.9 ±0.4

S - surface water; M - mid-depth water; B - bottom water.
a - Norwegian and Russian data (mean value (±SD)).
b - Russian data only.

4.3.2 Sr-90

The data reported by Norway and Russia for activity concentrations of Sr-90 for each seawater sample showed a clear disparity, even when taking into account the analytical uncertainties on the individual measurements (Table 4.1). Sampling of seawater in 2014 was carried out in a manner that was designed to minimise any inherent variation between samples collected from the same station and depth. However, data reported by Russia for Sr-90 was between 2.6 and 5.8 fold higher than Norwegian data for the same samples. Activity concentrations of Sr-90 reported by Russia for bottom water ranged from 1.9 to 5.0 Bq/m^3 compared to 0.69 to 1.07 Bq/m^3 for the samples analysed by Norway. For the Norwegian samples collected in 2014 there was a delay of approximately 2.5 years between their collection and analysis due to problems exporting the samples and issues with analytical capacity. However, the Norwegian samples were acidified to pH 2 shortly after their collection that should ensure that any Sr-90 remained in solution. In the 2012 JRNEG expedition, seawater samples were analysed for Sr-90 by Norway, Russia and the IAEA (Table 4.2). Although the data reported by Norway and Russia showed better agreement than was the case in 2014, data reported by Russia was up to 2.8 fold higher than Norwegian data for the same samples. Norwegian results from 2012 were within 0.8 to 1.2 fold of the values reported by IAEA. In the report of the joint expedition in 2012, mean values of Norwegian, Russian and IAEA data for each sample were reported for Sr-90 (JRNEG, 2014).

Activity concentrations of Sr-90 in seawater sampled from Barents Sea, Norwegian Sea and the North Sea in 2014 have been reported to be within the range of 0.8 to 1.6 Bq/m^3 (Skjerdal et al., 2017;

BfS/BMU, 2017), which would be in better agreement with Norwegian data for Sr-90 for the samples collected around K-159. It should be noted that activity concentrations of Sr-90 similar to these values were also reported by Norway and the IAEA for seawater sampled from the Pechora Sea during the JRNEG expedition in 2012 (Table 4.2). Closer to the study site, activity concentrations of Sr-90 from a transect of surface water stations taken in 2013 along the length of Kola Bay showed a reported Sr-90 activity concentration of 4.6 ±0.3 Bq/m^3 close to Murmansk, decreasing to 2.9 ±0.5 Bq/m^3 towards the entrance of Kola Bay (MMBI/ApN, 2015). These values show a greater similarity to the activity concentrations of Sr-90 reported by Russia for the samples collected around K-159 than the Norwegian data and may suggest that there is a source of Sr-90 further within Kola Bay. In the same study (MMBI/ApN, 2015), activity concentrations up to 69 ±11 Bq/m^3 were reported for seawater from Andreeva Bay, with values decreasing from 7.6 ±1.2 Bq/m^3 to 1.6 ±0.1 Bq/m^3 in a transect of coastal water from the entrance to Andreeva Bay towards Kola Bay. These results suggest that Andreeva Bay may be acting as a local source of Sr-90 to coastal water along the Kola Peninsula, but that this flux is then diluted through mixing processes with Barents Sea water flowing from the West as the coastal water is transported towards Kola Bay. The activity concentration of Sr-90 in surface water closest to Kola Bay as reported by MMBI/ApN (2015), is closer in agreement with Norwegian data for seawater samples collected around K-159 in 2014.

In comparison with other marine regions in 2014, both Norwegian and Russian data for activity concentrations of Sr-90 in seawater from the area around K-159 in 2014 were lower than mean values for waters in the Baltic Sea region (HELCOM, 2015).

Apart from global fallout, additional sources of Sr-90 to Barents Sea water arise from long-range ocean transport of authorised discharges of this radionuclide from European reprocessing plants at Sellafield (UK) and Cap la Hague (France) and Sr-90 from the Chernobyl Accident. Cs-137/Sr-90 activity ratios for the North Sea and Norwegian Sea in 2014 have been reported to be between 1.4 to 3.3 (BfS/BMU, 2015) and 1.5 to 2.7 (Skjerdal et al., 2017), respectively, while the global fallout ratio for Cs-137/Sr-90 based on fission yields has been reported as being 1.5 (UNSCEAR, 2000). Cs-137/Sr-90 activity ratios for seawater in the area around K-159 based on Norwegian data for Sr-90 ranged between 1.4 to 2.3 (Table 4.3) which would be in good agreement with the aforementioned values from the North Sea and Norwegian Sea for the same year. Cs-137/Sr-90 activity ratios for seawater in the area around K-159 based on Russian data for Sr-90 were lower, ranging between 0.33 to 0.81 (Table 4.3). Such Cs-137/Sr-90 activity ratios would suggest a local source of Sr-90 as has been discussed above. If this is the case, the local source is unlikely to be K-159 as according to Hosseini et al. (2017) the Cs-137/Sr-90 activity ratio for the nuclear inventory of K-159 is approximately 1:1 and there has been no indication of any increase of Cs-137 activity concentrations in seawater or sediment above values typical for the region (See sections 4.3.1 and 4.4.1).

It is clear that there is a need for further work to identify the reasons behind the disparity in analytical results reported by Norway and Russia for Sr-90 in seawater.

Table 4.2. Comparison of Norwegian, Russian and IAEA Sr-90 activity concentrations (Bq/m^3) in filtered seawater from the 2012 JRNEG expedition.

Station	Depth	Sr-90 (Bq/m^3) Norway (<1 µm)	Russia (<1 µm)	IAEA (<0.45 µm)
Pechora sea	S	1.41 ±0.15	2.1 ±0.7	1.11 ±0.09
	M	1.13 ±0.10	2.2 ±0.7	1.14 ±0.10
	B	0.78 ±0.09	2.2 ±0.6	0.96 ±0.07
Entrance to Stepovogo Fjord	S	3.73 ±0.29	6.7 ±1.8	-
	B	2.03 ±0.17	4.8 ±1.6	-
Outer part of Stepovogo Fjord	S	4.03 ±0.32	4.1 ±1.1	3.44 ±0.69
	B	2.18 ±0.19	3.5 ±1.1	1.82 ±0.20
Inner part of Stepovogo Fjord	S	3.77 ±0.30	5.9 ±1.2	3.24 ±0.19
	B	5.26 ±0.41	6.8 ±1.4	5.28 ±0.40

S - surface water; M - mid-depth water; B - bottom water.

Table 4.3. Cs-137/Sr-90 activity ratios in filtered seawater (<1 µm) from Station K-159 compared to other sampling stations.

Station	Depth	Cs-137/Sr-90[a] Norway[b]	Russia[c]
K-159	S	1.52 ±0.23	0.58 ±0.13
	M	-	-
	B	1.94 ±0.32	0.33 ±0.07
St.8	B	2.33 ±0.44	0.48 ±0.12
St.12	B	1.41 ±0.21	0.48 ±0.1
St.14	B	1.59 ±0.28	0.47 ±0.11
St.18	B	2.23 ±0.41	0.81 ±0.19

S - surface water; M - mid-depth water; B - bottom water.

a - Derived using activity concentrations for Cs-137 reported in table 4.1 (Activity ratios stated with propagated uncertainties).

b - Derived using Norwegian activity concentrations for Sr-90 reported in table 4.1.

c - Derived using Russian activity concentrations for Sr-90 reported in table 4.1.

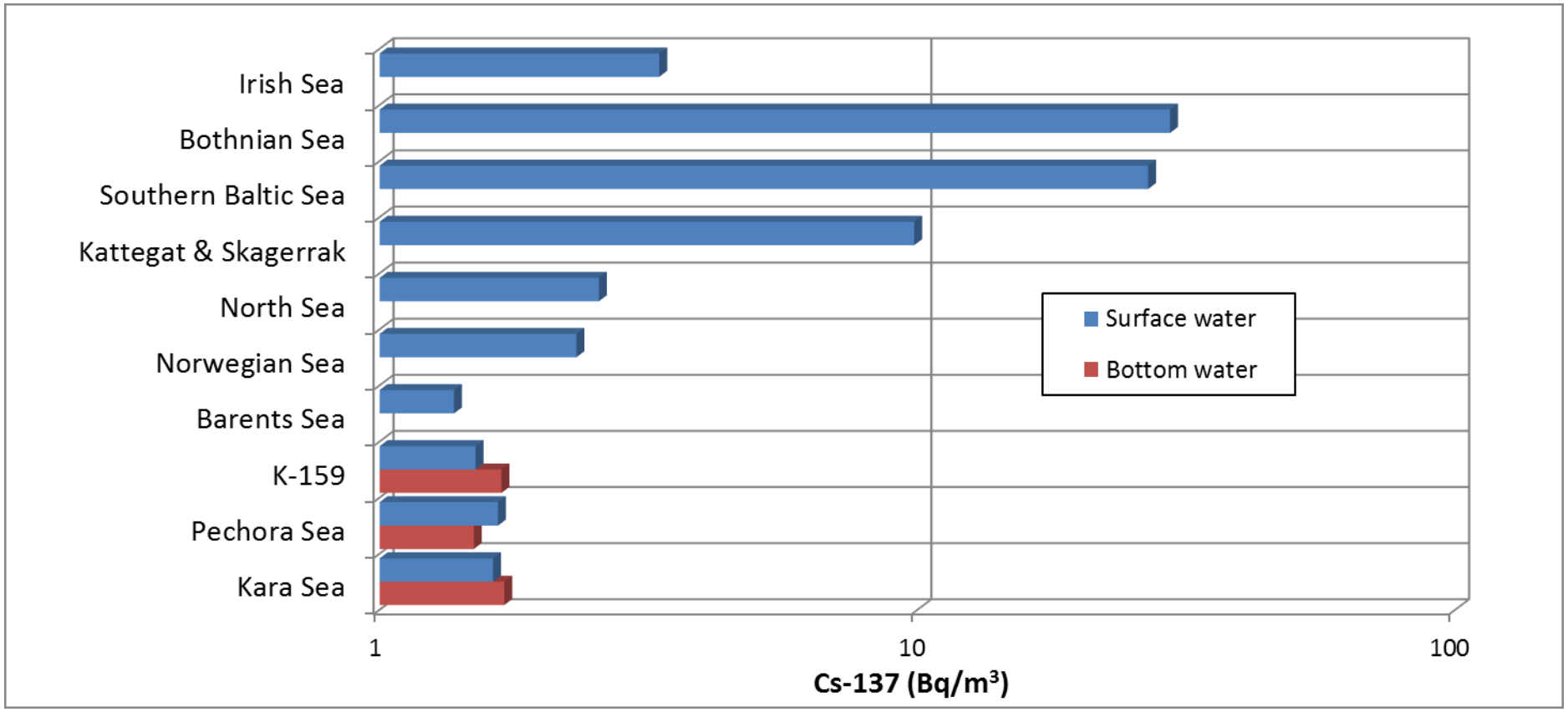

Figure 4.8. Comparison of mean Cs-137 activity concentrations (Bq/m^3) in filtered seawater (<1 µm) for Station K-159 (Norwegian and Russian data) with values for other seas (Note use of logarithmic scale for activity concentrations).

Irish Sea (2014) - mean activity concentration (EPA, 2016)
Bothnian Sea and Southern Baltic Sea (2014) - mean activity concentrations (HELCOM, 2015)
Kattegat & Skagerrak (2014) - mean activity concentration (Skjerdal et al., 2017)
North Sea (2014) - mean activity concentration (BfS/BMU, 2017)
Norwegian Sea (2014) - mean activity concentration (Skjerdal et al., 2017)
Barents Sea (2014) - mean activity concentration (Skjerdal et al., 2017)
Pechora Sea and Kara Sea (2012) - mean activity concentrations (JNREG, 2014)

4.3.3 Pu isotopes

The activity concentrations of Pu-239,240 observed at different sampling depths in <1 µm filtered seawater at Station K-159 increased from 2.2 ±1.0 mBq/m^3 in surface water to 6.9 ±1.1 mBq/m^3 in bottom water (Table 4.4). This value for Pu-239,240 in in <1 µm filtered bottom water near K-159 was within the range of values (5.9 to 15.2 mBq/m^3) for <1 µm filtered bottom water from the other sampling stations. The highest activity concentration of Pu-239,240 in <1 µm filtered seawater was observed at Station 18, to the south of K-159. The activity concentrations of Pu-239,240 observed in <0.45 µm filtered seawater from all depths at Station K-159 and in <0.45 µm filtered bottom water from all other stations were similar with a range of 2.7 to 5.0 mBq/m^3 (Table 4.4). Activity concentrations of Pu-239,240 in <1 µm and <0.45 µm filtered seawater from Stations K-159 and 8 were similar, whereas activity concentrations of Pu-239,240 in <0.45 µm filtered bottom water from Stations 12, 14 and 18 were 2 to 3 fold lower than for <1 µm filtered samples. The activity concentrations of Pu-239,240 in suspended matter (>1 µm) at Station K-159 increased from 0.5 ±0.2 mBq/m^3 in surface water to 2.3 ±0.5 mBq/m^3 in bottom water with values ranging from 1.1 to 3.8 mBq/m^3 for all other stations (Table 4.4).

Pu-240/Pu-239 atomic ratios in <0.45 µm filtered seawater samples (Table 4.5) ranged between 0.172 to 0.190 which were in good agreement with a value of 0.180 ± 0.014 for global fallout in northern regions (Kelley et al., 1999).

The range of Pu-239,240 activity concentrations in <1 µm filtered seawater from the sampling area in 2014 were in general higher than previously reported values in seawater sampled in the Pechora Sea and Kara Sea during the JNREG expedition in 2012, although activity concentrations in <0.45 µm filtered seawater were similar (JNREG, 2014). Activity concentrations of Pu-239,240 in suspended matter from the sampling area in 2014 were in general an order of magnitude higher than those observed for suspended matter from the Pechora Sea and Kara Sea (JNREG, 2014).

In comparison with other marine regions (Figure 4.9), the Pu-239,240 activity concentrations in <1 µm filtered seawater from Station K-159 was similar to reported mean values in 2014 for the Barents Sea, Norwegian Sea and North Sea (Skjerdal et al., 2017; BfS/BMU, 2017), but lower than a value reported in 2011 for the Bothnian Sea (HELCOM, 2015).

Taking all data into consideration, the relative contributions of Pu-239,240 activity concentrations in the different size fractions of seawater from the sampling area showed that Pu-239,240 had a greater association with size fractions >0.45 µm in bottom water than compared to surface or mid-depth water. In surface water, practically all (99%) Pu-239,240 was associated with the <0.45 µm fraction, whereas in bottom water only 23% to 54% of Pu-239,240 was associated with this size fraction. The presence of suspended matter was evident from the video surveillance of K-159 with the ROV and is likely to originate from terrestrial run off and out flowing waters from Kola Bay. From such observations, it could be inferred that the area may act as a sink for particle reactive radionuclides such as Pu-239,240, although the influence of lower salinity coastal water in bottom waters (as described in section 4.1) may potentially allow for the remobilization of particulate bound Pu-239,240.

Table 4.4. Pu-239,240 activity concentrations (mBq/m^3) in different size fractions of seawater from Station K-159 compared to other sampling stations.

Station	Depth	Pu-239,240 (mBq/m^3)		
		>1 µm[a]	<1 µm[a]	<0.45 µm[b]
K-159	S	0.5 ±0.2	2.2 ±1.0	2.7 ±0.1
	M	1.7 ±0.6	4.7 ±1.1	4.1 ±0.1
	B	2.3 ±0.5	6.9 ±1.1	5.0 ±0.1
St.8	B	3.8 ±1.0	5.9 ±2.3	3.7 ±0.1
St.12	B	2.6 ±0.7	8.9 ±2.8	4.0 ±0.1
St.14	B	1.1 ±0.4	10.3 ±0.5	4.6 ±0.1
St.18	B	2.6 ±0.5	15.2 ±4.3	4.1 ±0.1

S - surface water; M - mid-depth water; B - bottom water.
a - Russian data.
b - Norwegian data.

Table 4.5. Pu-240/Pu-239 atomic ratios in filtered seawater (<0.45 µm) from Station K-159 compared to other sampling stations.

Station	Depth	Pu-240/Pu-239[a]
K-159	S	0.189 ±0.016
	M	0.188 ±0.014
	B	0.172 ±0.010
St.8	B	0.173 ±0.013
St.12	B	0.184 ±0.013
St.14	B	0.174 ±0.010
St.18	B	0.190 ±0.013

S - surface water; M - mid-depth water; B - bottom water.
a - Norwegian data (Atomic ratios stated with propagated uncertainties).

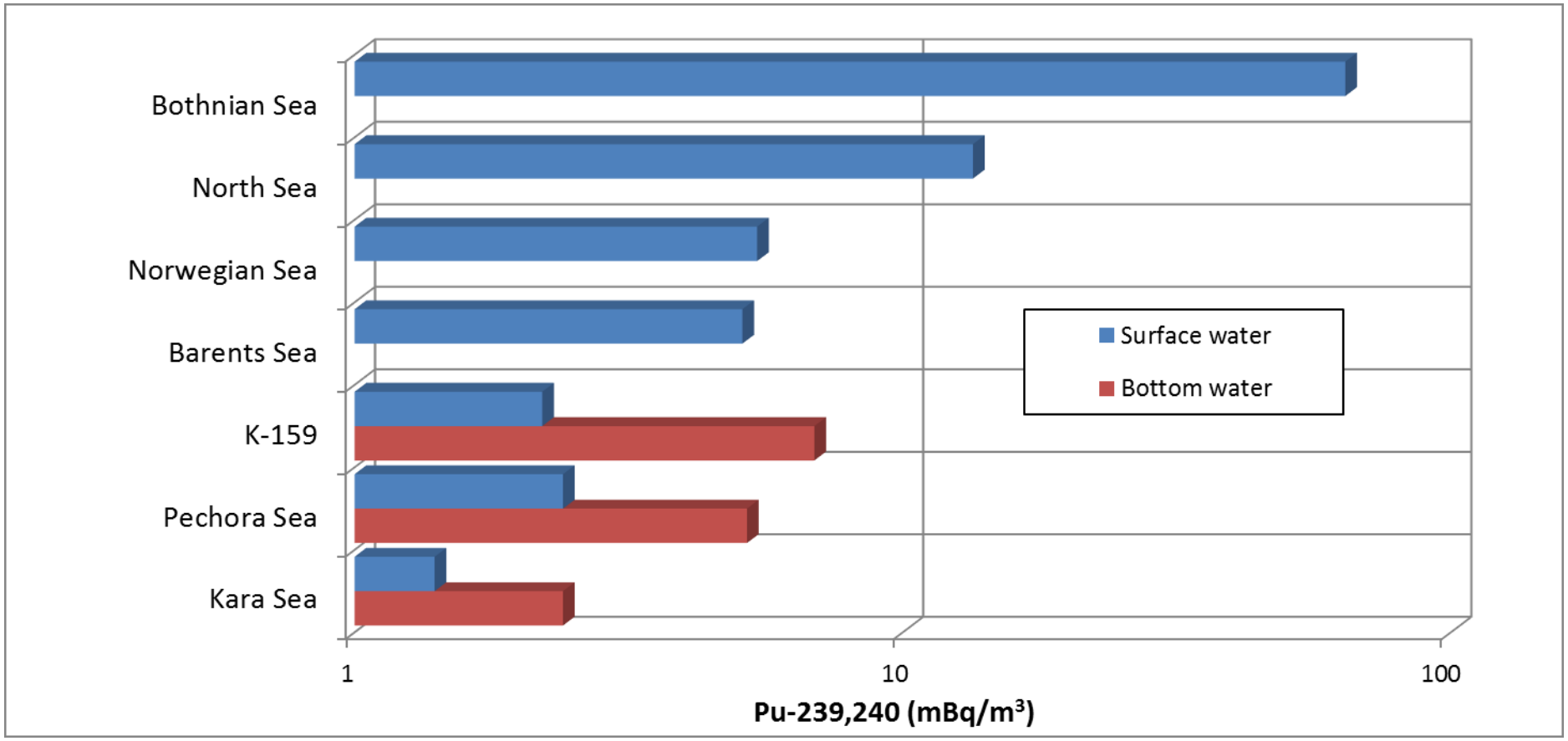

Figure 4.9 Comparison of Pu-239,240 activity concentrations (mBq/m³) in filtered seawater (<1 µm) from Station K-159 (Russian data) with values for other seas (Note use of logarithmic scale for activity concentrations).

Bothnian Sea (2011) - single reported activity concentration (HELCOM, 2015).
North Sea (2014) - mean activity concentration (BfS/BMU, 2017).
Norwegian Sea (2014) - mean activity concentrations (Skjerdal et al., 2017).
Barents Sea (2014) - single reported activity concentration (Skjerdal et al., 2017).
Pechora Sea and Kara Sea (2012) - mean activity concentrations (JNREG, 2014).

4.3.5 H-3

The activity concentration of H-3 in filtered bottom seawater collected near K-159 was 0.66 ±0.06 kBq/m^3 which was similar to values for all other sampling depths and stations at between 0.24 and 0.59 kBq/m^3 (Table 4.6). The H-3 activity concentrations in seawater from the sampling area in 2014 were lower than previously reported values for seawater sampled in the Kara Sea during the JNREG expedition in 2012 but comparable to those in the Pechora Sea (JNREG, 2014), as well as to open sea values from 2011 for the North Sea (BfS/BMU, 2014).

4.3.6 I-129

The concentration of I-129 in filtered bottom seawater collected near K-159 was 87 ±10.2 x 10^8 atoms/l which was similar to values for all other sampling depths and stations at between 73 and 104 x 10^8 atoms/l (Table 4.6). The I-129 concentrations in seawater from the sampling area in 2014 were comparable to previously reported values for seawater sampled in the Pechora Sea and Kara Sea during the JNREG expedition in 2012 (JNREG, 2014). These concentrations are significantly higher than the range (9 to 25 x 10^8 atoms/l) reported for surface waters from the Barents and Kara Seas in the 1990s (Raisbeck et al., 1993). The elevated level of I-129 concentrations can be accounted for by the long range transport of increased discharges of this radionuclide in recent years from the nuclear reprocessing facilities at Sellafield and in particular Cap la Hague (Hou et al., 2009).

Table 4.6. H-3 activity concentrations (kBq/m^3) in filtered seawater (<1 µm) and I-129 concentrations (x 10^8 atoms/l) in filtered seawater (<0.45 µm) from Station K-159 compared to other sampling stations.

Station	Depth	H-3 (kBq/m^3)[a]	I-129 (x 10^8 atoms/l)[b]
K-159	S	0.47 ±0.08	100 ±1.4
	M	0.59 ±0.08	73 ±0.8
	B	0.66 ±0.06	87 ±10.2
St.8	B	0.46 ±0.05	104 ±1.4
St.12	B	0.24 ±0.04	89 ±10.1
St.14	B	0.40 ±0.05	75 ±0.4
St.18	B	0.37 ±0.05	99 ±0.6

S - surface water; M - mid-depth water; B - bottom water.
a - Russian data.
b - Norwegian data.

4.3.7. Trace elements

Trace element data can provide useful site specific insights into the behaviour and occurrence of their radioactive counterparts allowing for more accurate predictions of the consequences of any hypothetical releases from K-159. Furthermore, an understanding of concentrations of potentially toxic elements is of importance in a multiple stressor context.

The relatively high concentration of Cd, Cu, Fe, Ni and Pb observed in seawater from mid-depth water at Station K-159 (Table 4.7) are probably derived from terrestrial sources and demonstrate the influence of coastal run-off on the local oceanography. In general, the relative distribution in the concentrations of the trace elements between different size class fractions across the different sampling stations was similar. The processes controlling the speciation of these trace elements in the

sampling area around K-159 might also affect the speciation of radionuclides. Mean U-235/U-238 atomic ratios for all samples and all fractions (0.0065 - 0.0077) were in good agreement with the expected atomic ratio of 0.0073 for natural uranium.

Table 4.7. Mean (±SD) concentration of selected trace elements in seawater from Station K-159 compared to other sampling stations.

Trace element[a]		K-159			St.8	St.12	St.14	St.18
		S	M	B	B	B	B	B
Mn	Unfiltered	0.9±0.1	0.5±0.1	0.4±0.0	0.3±0.1	0.4±0.1	0.5±0.1	0.4±0.1
(µg/l)	<0.45 µm	0.8±0.1	0.4±0.1	0.4±0.0	0.3±0.1	0.4±0.1	0.5±0.1	0.4±0.1
	<10 kDa	0.6±0.0	0.6±0.1	0.4±0.1	0.4±0.0	0.3±0.1	0.5±0.0	0.4±0.0
Fe	Unfiltered	1.5±0.4	5.7±0.8	1.4±0.9	0.7±0.1	0.7±0.2	1.9±2.1	2.1±0.8
(µg/l)	<0.45 µm	4.8±5.9	5.6±0.8	1.4±1.0	0.7±0.1	0.7±0.2	1.9±2.1	2.0±0.8
	<10 kDa	0.5±0.1	3.5±2.8	1.4±0.9	2.3±0.5	2.8±3.4	0.5±0.9	2.1±0.4
Co	Unfiltered	0.10±0.02	0.02±0.00	0.01±0.01	0.01±0.00	0.13±0.07	0.04±0.02	0.04±0.04
(µg/l)	<0.45 µm	0.10±0.02	0.02±0.00	0.01±0.01	0.01±0.00	0.13±0.07	0.04±0.02	0.04±0.04
	<10 kDa	0.01±0.00	0.02±0.00	0.01±0.00	0.01±0.00	0.01±0.00	0.01±0.00	0.01±0.00
Ni	Unfiltered	0.4±0.0	1.4±0.1	0.2±0.1	0.2±0.0	0.2±0.0	0.2±0.0	0.2±0.0
(µg/l)	<0.45 µm	0.4±0.0	1.4±0.1	0.2±0.1	0.2±0.0	0.2±0.0	0.2±0.0	0.2±0.0
	<10 kDa	0.3±0.0	1.3±0.2	0.2±0.0	0.2±0.0	0.3±0.0	0.2±0.0	0.2±0.0
Cu	Unfiltered	0.4±0.0	1.9±0.2	0.5±0.3	0.2±0.0	0.2±0.0	0.2±0.0	0.2±0.1
(µg/l)	<0.45 µm	0.4±0.0	1.9±0.2	0.5±0.3	0.2±0.0	0.2±0.0	0.2±0.0	0.2±0.1
	<10 kDa	0.2±0.1	1.6±0.2	0.2±0.0	<0.2	<0.2	<0.2	<0.2
Sr	Unfiltered	7.1±0.6	7.8±0.3	8.1±0.8	7.5±0.8	7.5±0.8	7.6±0.6	6.7±0.4
(mg/l)	<0.45 µm	6.8±0.6	7.6±0.3	8.3±0.8	7.7±0.8	7.5±0.8	7.6±0.6	6.5±0.4
	<10 kDa	7.2±0.2	7.4±0.8	7.7±1.1	8.7±0.1	8.0±0.2	7.8±0.6	7.2±0.8
Cd	Unfiltered	0.008±0.005	16.6±0.5	0.020±0.005	0.013±0.005	0.013±0.005	0.015±0.005	0.013±0.003
(µg/l)	<0.45 µm	0.008±0.005	16.5±0.5	0.020±0.005	0.013±0.005	0.013±0.005	0.015±0.005	0.013±0.003
	<10 kDa	0.008±0.005	16.0±1.6	0.022±0.005	0.014±0.000	0.019±0.008	0.011±0.004	0.019±0.005
Cs	Unfiltered	0.3 ±0.0	0.3 ±0.0	0.3 ±0.0	0.3 ±0.0	-	0.3 ±0.0	0.3 ±0.0
(µg/l)	<0.45 µm	0.3 ±0.0	0.3 ±0.0	0.3 ±0.0	0.3 ±0.0	0.3 ±0.0	0.3 ±0.0	0.3 ±0.0
	<10 kDa	0.3 ±0.0	0.3 ±0.0	0.3 ±0.0	0.3 ±0.0	0.3 ±0.0	0.3 ±0.0	0.3 ±0.0
Pb	Unfiltered	0.6±0.4	5.9±0.2	0.4±0.3	0.7±0.0	1.3±0.1	0.4±0.1	0.6±0.0
(µg/l)	<0.45 µm	0.7±0.4	6.1±0.3	0.4±0.3	0.7±0.0	1.3±0.1	0.4±0.1	0.6±0.0
	<10 kDa	0.4±0.1	0.1±0.0	0.7±0.0	0.1±0.0	0.1±0.0	0.1±0.1	0.1±0.1
U	Unfiltered	2.6±0.3	2.9±0.1	3.8±0.2	3.2±0.3	2.9±0.3	2.9±0.2	2.6±0.2
(µg/l)	<0.45 µm	2.8±0.4	2.9±0.1	3.7±0.5	3.1±0.5	2.9±0.4	2.8±0.2	2.5±0.1
	<10 kDa	2.9±0.0	3.0±0.3	3.7±0.4	3.5±0.3	3.1±0.0	2.9±0.2	2.8±0.4

S - surface water; M - mid-depth water; B - bottom water.

a - Norwegian data.

Unfiltered (n=2); <0.45 µm and <10 kDa (n=3), except for Cs (n=2). Where SD is given as 0.0, 0.00 and 0.000, SD was less than 0.5, 0.05 and 0.005, respectively. Uncertainties on individual measurements were typically between 2% and 5%.

4.4 Radionuclides and trace elements in sediments

4.4.1 Cs-137

The mean activity concentrations of Cs-137 in surface sediments collected with the ROV (Table 4.8) at locations near the bow, stern and either side of the rector compartment of K-159 were between 0.7 and 3.2 Bq/kg (d.w.). These values were similar to the activity concentration in surface sediment observed at Station K-159 (3.0 ±0.7 Bq/kg (d.w.)) and all other stations around K-159 (<0.2 to 5.0 Bq/kg (d.w.)) (Table 4.9).

The activity concentrations of Cs-137 surface sediments observed in 2014 show good agreement for reported values (<0.8 to 4.6 Bq/kg d.w.) for sediments collected close to K-159 in 2007 (Hosseini et al., 2017). Activity concentrations of Cs-137 in surface sediments within the range of values observed for the sampling area in 2014 have been reported previously for the local region (Leppänen et al., 2013; MMBI/ApN, 2015) and for the Pechora Sea and Kara Sea in sediments sampled during the JNREG expedition in 2012 (JNREG, 2014). In comparison with other marine regions (Figure 4.10), the Cs-137 activity concentrations in surface sediments from the sampling area were similar to recently reported values for the Barents Sea, Norwegian Sea and North Sea (Skjerdal et al., 2017), but lower than values for 2014 for the Baltic Sea region (HELCOM, 2015) and UK coastal sediments from the Irish Sea (RIFE, 2015).

The activity concentrations of Cs-137 in a sediment core from Station K-159 (Figure 4.11) showed a sub-surface peak at a depth of 2 to 3 cm of 4.4 ±0.5 Bq/kg (d.w.), with activity concentrations decreasing to less than surface values below a depth of 6 cm to a minimum of 1.2 ±0.3 Bq/kg (d.w.). Activity concentrations of Cs-137 in cores from all other sampling stations (Figure 4.12) typically showed similar profiles, i.e. with sub-surface peaks, to the core from Station K-159. In seven cores, the sub-surface peak in Cs-137 activity concentrations occurred in the top 4 cm, while deeper sub-surface peaks between 5 and 12 cm were observed in the other 5 cores. The maximum Cs-137 activity concentration observed in any of the cores sampled was 8.4 ±1.1 Bq/kg (d.w.).

Assuming that local sedimentation rates have remained reasonably constant, the observation of sub-surface peaks in Cs-137 activity concentrations across the sampling area suggests that fluxes of Cs-137 to the sediment were greater in the past than at present. This observation could support the idea that main source of Cs-137 to the area is derived from long-range ocean transport, with the decrease in fluxes to sediments over time reflecting the reductions in contributions from sources such as global fallout and discharges of this radionuclide from nuclear reprocessing facilities at Sellafield (UK) and Cap la Hague (France).

The Cs-137 sediment inventory to a depth of 12 cm at Station K-159 was 224 ±10 Bq/m^2, which was within the range of sediment inventories for core depths between 10 and 22 cm for the other sampling stations of 203 to 722 Bq/m^2 (Table 4.10). For comparison, the Cs-137 sediment inventory for a 12 cm core from the Pechora Sea sampled during the JNREG expedition in 2012 was 581 ±25 Bq/m^2 (JNREG, 2014). The distribution of available data for Cs-137 sediment inventories in the top 10 cm across the sample area suggests that fluxes of Cs-137 have been higher to sediments in deeper areas to the west of K-159, compared to sediments at shallower depths to the east. This probably reflects the prevailing sedimentation dynamics (deposition and remobilisation) and transport of fine sediments from shallower to deeper waters in the sample area. From the investigations in 2007, sediments in the area were reported to be 50% clay, 40% silt and 10% sand (Sarkisov et al., 2009). In cores that were at least

18 cm deep, the percentage of the total Cs-137 inventory that was deeper than 10 cm deeper was between 9.4% and 48.9%.

No other gamma emitting anthropogenic radionuclides were detected in any sediment sample.

Table 4.8. Cs-137 and Sr-90 activity concentrations (Bq/kg d.w.) in surface sediments collected by ROV at locations close to the outer hull of K-159.

Sample	Location around K-159	Cs-137[a] (Bq/kg d.w.)	Sr-90[b] (Bq/kg d.w.)
ROV 1	Bow	1.7 ±0.2	1.5 ±0.3
ROV 2	Starboard reactor	0.9 ±0.1	2.6 ±0.5
ROV 3	Stern	0.7 ±0.2	1.0 ±0.2
ROV 4	Port reactor	3.2 ±1.0	2.7 ±0.6

a - Norwegian and Russian data (mean value (±SD)).
b - Russian data.
Uncertainties on all individual measurements were typically 20%.

Table 4.9. Cs-137 and Sr-90 activity concentrations (Bq/kg d.w.) in surface sediment from Station K-159 compared to surface sediments from other stations.

	K-159 (Bq/kg d.w.)	Other stations (Bq/kg d.w.)		
		n	Mean (±SD)	Range
Cs-137[a]	3.0 ±0.7	16	2.8 ±1.2	<0.2 - 5.0
Sr-90[a]	1.4 ±0.3	16	1.5 ±0.9	0.5 - 3.7

a - Russian data.
Uncertainties on all individual measurements were typically 20% or less. n - number of sampling stations.

Table 4.10. Inventory for Cs-137 (Bq/m^2 d.w.) in sediment core from Station K-159 compared to inventories in sediment cores from other stations.

	n	Core depth (cm)	Cs-137[a] (Bq/m^2 d.w.)	
			Mean (±SD)	Range
K-159	1	12	224 ±10	-
Other stations	11	10-22	389 ±174	203 - 722

a - Russian data.
n - number of sampling stations.

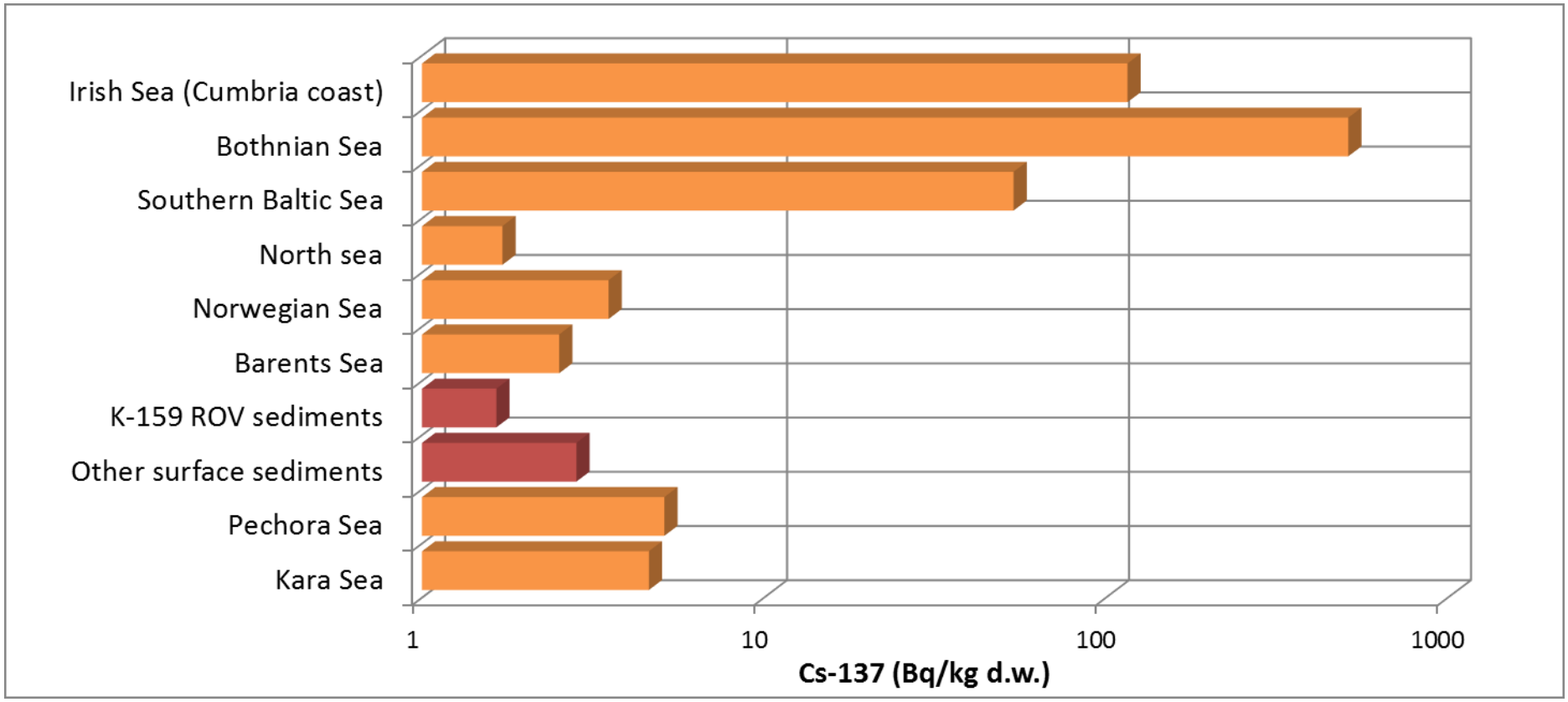

Figure 4.10. Comparison of mean surface sediment Cs-137 activity concentrations (Bq/kg d.w.) from this study (Norwegian and Russian data) with values for other seas (Note use of logarithmic scale for activity concentrations).

Irish Sea, Cumbria coast (2014) - mean activity concentrations (RIFE, 2015).

Bothnian Sea and Southern Baltic Sea (2014) - mean activity concentrations (HELCOM, 2015).

North Sea (2013), Norwegian Sea (2014) and Barents Sea (2012) - mean activity concentrations (Skjerdal et al., 2017).

Pechora Sea and Kara Sea (2012) - mean activity concentrations (JNREG, 2014).

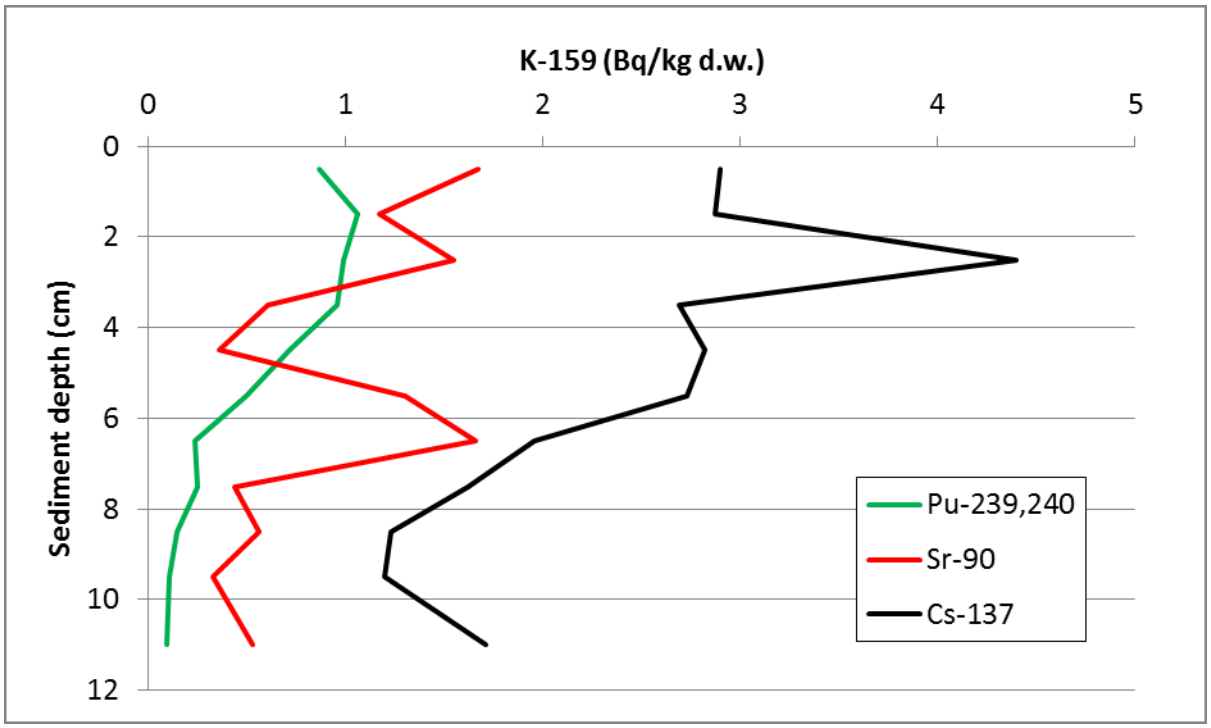

Figure 4.11. Cs-137, Sr-90 and Pu-239,240 activity concentrations (Bq/kg d.w.) in a sediment core from station K-159 (Russian data). Uncertainties on individual measurements were typically 20% or less.

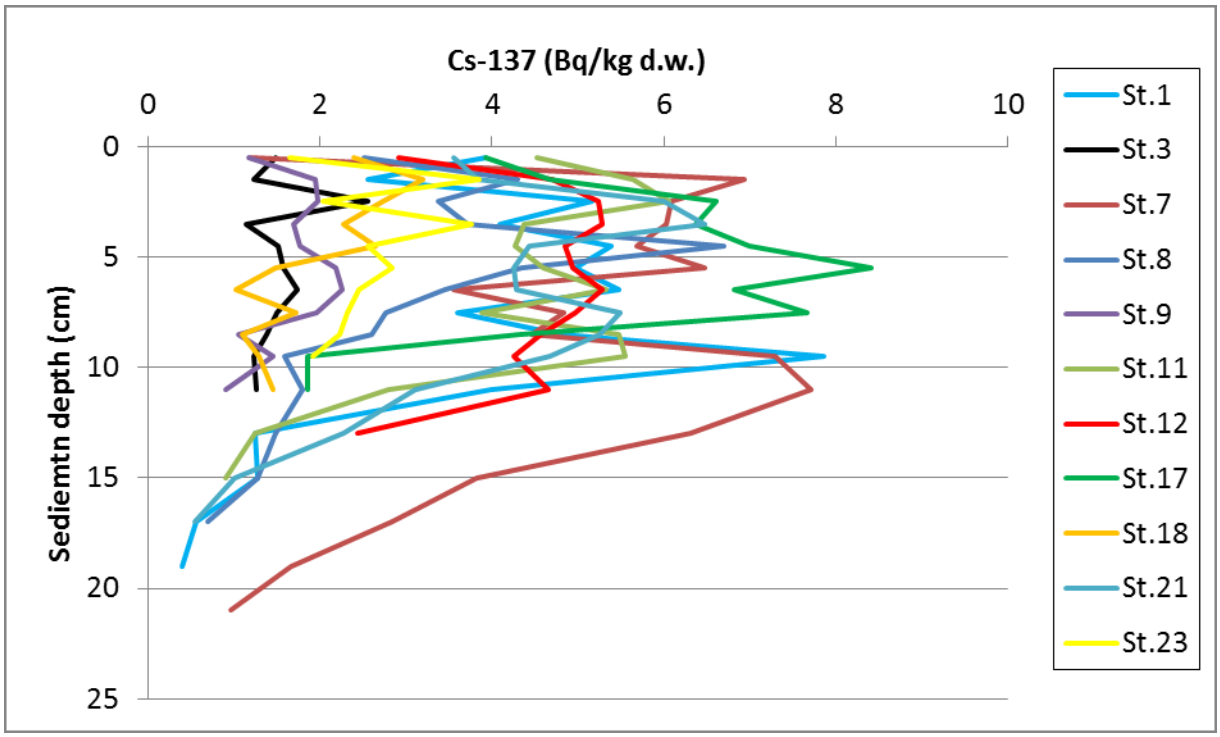

Figure 4.12. Cs-137 activity concentrations (Bq/kg d.w.) in sediment cores from sampled stations (Russian data). Uncertainties on individual measurements were typically 20%.

4.4.2 Sr-90

The activity concentrations of Sr-90 in surface sediments collected with the ROV (Table 4.8) at locations near the bow, stern and either side of the rector compartment of K-159 were between 1.0 and 2.7 Bq/kg (d.w.). These values were similar to the activity concentration in surface sediment observed at Station K-159 (1.4 ±0.3 Bq/kg (d.w.)) and all other stations (0.5 to 3.7 Bq/kg (d.w.)) (Table 4.8). No particular trend could be seen in the distribution of Sr-90 activity concentrations surface sediments across the sample area based on the samples taken.

Activity concentrations of Sr-90 in surface sediments within the range of values observed for the sampling area in 2014 have been reported previously for the local region (Leppänen et al., 2013; MMBI/ApN, 2015) and for the Pechora Sea during the JNREG expedition in 2012 (JNREG, 2014). In contrast, the Sr-90 activity concentrations in surface sediments from the sampling area in 2014 were typically an order of magnitude higher than those observed in the Kara Sea (JNREG, 2014).

The activity concentrations of Sr-90 in a sediment core from Station K-159 (Figure 4.11) showed an alternating profile. Minimums could be observed at a depth of 4 to 5 cm and below 7 cm, while the activity concentrations between 5 and 7 cm were similar to values in the surface layers of the core. The activity concentrations of Sr-90 in selected slices of cores from Stations 7, 8 and 17 were typically less than 1 Bq/kg (d.w.), while for Stations 12 and 18, values were typically more than 2 Bq/kg (d.w.) at various depths, up to a maximum of 4.8 ±1.0 Bq/kg (d.w.). For comparison, these values are an order of magnitude lower than mean values reported for UK coastal sediments in 2014 from the Irish Sea (RIFE, 2015). The data available on the depth distributions of Sr-90 in sediment from the sampling area suggest that fluxes of Sr-90 have fluctuated in the past.

The Sr-90 sediment inventory to a depth of 12 cm at Station K-159 was 85 ±6 Bq/m^2, while the data available for selected slices in cores from Stations 12 and 18 would indicate inventories more than twice this value. Cs-137/Sr-90 activity ratios in surface sediments and cores were typically greater than 1, with higher values in surface sediments in deeper areas to the west of K-159 compared to shallower depths to the east. These observations reflect the relatively higher particle reactivity of Cs-137 compared to Sr-90 and the differences in Cs-137 fluxes to sediments across the sampling area.

4.4.4 Pu isotopes and Am-241

The activity concentrations of Pu-239,240 in surface sediments collected with the ROV (Table 4.11) at locations near the bow, stern and either side of the rector compartment of K-159 were between 0.13 and 1.17 Bq/kg (d.w.). These values were similar to the activity concentration in surface sediment observed at Station K-159 (0.45 ±0.07 Bq/kg (d.w.)) and all other stations (0.28 to 1.83 Bq/kg (d.w.)) (Table 4.11). The distribution of Pu-239,240 activity concentrations in the sample area based on the samples taken suggests a similar picture to Cs-137 with a general trend of higher activity concentrations in surface sediments in deeper areas to the west of K-159 compared to shallower depths to the east.

Activity concentrations of Pu-239,240 in surface sediments within the range of values observed for the sampling area in 2014 have been reported previously in sediments sampled in the Pechora Sea and Kara Sea during the JNREG expedition in 2012 (JNREG, 2014). For comparison, these values are up to 2 orders of magnitude lower than mean values reported for UK coastal sediments in 2014 from the Irish Sea (RIFE, 2015).

The activity concentrations of Pu-239,240 in a sediment core from Station K-159 (Figure 4.11) showed a slight sub-surface peak at a depth of 1 to 2 cm of 1.06 ±0.12 Bq/kg (d.w.), with activity concentrations decreasing to less than surface values below a depth of 4 cm to a minimum of 0.10 ±0.02 Bq/kg (d.w.). Based on data available for this one core, the observation of higher Pu-239,240 activity concentrations in surface sediments than deeper sediments may suggest that fluxes of Pu-239,240 to sediment in the sampling area have been somewhat higher in more recent years than earlier.

The Pu-239,240 sediment inventory to a depth of 12 cm at Station K-159 was 46 ±2 Bq/m^2, which is approximately 3 fold lower than the inventory derived for the same depth of sediment for a core sampled in the Pechora Sea during the JNREG expedition in 2012 (JNREG, 2014).

Activity ratios of Pu-238/Pu-239,240 in surface sediments collected with the ROV (Table 4.13) at locations near the bow, stern and either side of the rector compartment of K-159 were between 0.036 and 0.081. Based on earlier work by Hardy et al. (1973) and allowing for the decay of Pu-238, expected 2014 global fallout activity ratios of Pu-238/Pu-239,240 between 60 and 70˚N would be 0.028 ±0.022. Due to the associated uncertainties on the activity ratios for these samples, it is difficult to draw any firm conclusions as to the source(s) of Pu isotopes observed in the sediments collected next to K-159. Other possible sources of Pu isotopes, such as long-range transport of discharges from European reprocessing plants, have been shown to have Pu-238/Pu-239,240 activity ratios an order of magnitude higher than global fallout (e.g. Morris et al., 2000; Oughton et al., 1999). Contributions of Pu isotopes from such sources to the sampling area would result in higher Pu-238/Pu-239,240 activity ratios than would be expected from global fallout alone.

The activity concentrations of Am-241 in surface sediments collected with the ROV (Table 4.11) at locations near the bow, stern and either side of the rector compartment of K-159 were between 0.07 and 0.43 Bq/kg (d.w.). Activity concentrations of Am-241 in surface sediments within the range of values observed for the sampling area in 2014 have been reported previously in sediments sampled in the Pechora Sea and Kara Sea during the JNREG expedition in 2012 (JNREG, 2014). For comparison, these values are up to 4 orders of magnitude lower than mean values reported for UK coastal sediments in 2014 from the Irish Sea (RIFE, 2015).

Activity ratios of Am-241/Pu-239,240 in surface sediments collected with the ROV (Table 4.13) at locations near the bow, stern and either side of the rector compartment of K-159 were between 0.41 and 0.74. From the activity ratio of Pu-241/Pu-239,240 in global fallout (UNSCEAR, 1993), the latitudinal distributions of Pu-239,240 (Hardy et al., 1973) and the ingrowth of Am-241 from Pu-241, an Am-241/Pu-239,240 activity ratio of 0.42 can be derived between 60 and 70˚N for global fallout. Due to the associated uncertainties on the activity ratios for these samples, it is difficult to draw any firm conclusions. In marine systems, this activity ratio can be disturbed due to the higher particle reactivity of Am-241 compared to Pu isotopes, additional sources of Am-241 and/or Pu-239,240 and the ingrowth of Am-241 from other sources of anthropogenic Pu-241 in the environment.

Pu-240/Pu-239 atomic ratios in in surface sediments collected with the ROV (Table 4.13) at locations near the bow, stern and either side of the rector compartment of K-159 were between 0.187 and 0.194. These ratios are in good agreement with the values observed in <0.45 µm filtered seawater samples (Table 4.5) and with a value of 0.180 ± 0.014 for global fallout in northern regions (Kelley et al., 1999).

Table 4.11. Pu-238, Pu-239,240 and Am-241 activity concentrations (Bq/kg d.w.) in surface sediment collected by ROV at locations close to the outer hull of K-159.

Sample	Location around K-159	Pu-238[a] (Bq/kg d.w.)	Pu-239,240[a] (Bq/kg d.w.)	Am-241[a] (Bq/kg d.w.)
ROV 1	Bow	0.032 ±0.011	0.88 ±0.08	0.43 ±0.06
ROV 2	Starboard reactor	<0.014	0.13 ±0.03	0.07 ±0.02
ROV 3	Stern	0.012 ±0.009	0.15 ±0.03	0.11 ±0.02
ROV 4	Port reactor	0.054 ±0.016	1.17 ±0.11	0.48 ±0.05

a – Norwegian data (Russian data showed broadly similar values but data was only available for Pu-239,240).

Table 4.12. Pu-239,240 activity concentrations (Bq/kg d.w.) in surface sediment from Station K-159 compared to surface sediments from other stations.

	K-159 (Bq/kg d.w.)	Other stations (Bq/kg d.w.)		
		n	Mean (±SD)	Range
Pu-239,240[a]	0.45 ±0.07	16	1.02 ±0.56	0.28 - 1.83

a - Russian data.
n - number of sampling stations.
Uncertainties on all individual measurements were typically 20% or less.

Table 4.13. Pu-238/Pu-239,240 and Am-241/Pu-239,240 activity ratios and Pu-240/Pu-239 atomic ratios in surface sediment collected by ROV at locations close to the outer hull of K-159.

Sample	Location around K-159	Pu-238/Pu-239,240[a]	Am-241/Pu-239,240[a]	Pu-240/Pu-239[a]
ROV 1	Bow	0.036 ±0.013	0.49 ±0.08	0.188 ±0.015
ROV 2	Starboard reactor	-	0.52 ±0.18	0.187 ±0.017
ROV 3	Stern	0.081 ±0.062	0.74 ±0.21	0.194 ±0.016
ROV 4	Port reactor	0.046 ±0.014	0.41 ±0.06	0.191 ±0.015

a – Norwegian data (Activity ratios and atomic ratios stated with propagated uncertainties).

4.4.5 I-129

Concentrations of I-129 in surface sediments collected with the ROV (Table 4.14) at locations near the bow, stern and either side of the rector compartment of K-159 were between 77 and 190 x 10^{11} atoms/kg (d.w.).These values are comparable to concentrations of I-129 reported for sediments from the Baltic Sea (Aladahan et al., 2007) and Kattegat (Lopez-Guitierrez et al., 2004), but an order of magnitude lower than a reported value (4800 x 10^{11} atoms/kg d.w.) from a sample of sediment taken from the Irish Sea (Hou et al. 2003).

Table 4.14. I-129 concentrations (x 10^{11} atoms/kg d.w.) in surface sediment collected by ROV at locations close to the outer hull of K-159.

Sample	Location around K-159	I-129[a] (x 10^{11} atoms/kg d.w.)
ROV 1	Bow	120 ±1.5
ROV 2	Starboard reactor	77 ±1.3
ROV 3	Stern	120 ±1.6
ROV 4	Port reactor	190 ±2.5

a – Norwegian data.

4.4.6 Trace elements

In general, concentrations of trace elements in sediments collected with the ROV (Table 4.15) at locations near the bow, stern and either side of the rector compartment of K-159 were similar. Mean U-235/U-238 atomic ratios for these sediment samples (0.0071 - 0.0075) were in good agreement with the expected atomic ratio of 0.0073 for natural uranium.

Table 4.15. Mean (±SD) concentration of selected trace elements (µg/g) in surface sediments collected by ROV at locations close to the outer hull of K-159.

Sample	Location around K-159	Trace elements[a] Mn (µg/g)	Fe (µg/g)	Co (µg/g)	Sr[b] (µg/g)	Cs (µg/g)	I (µg/g)	U (µg/g)
ROV 1	Bow	365±7	37.5±1.2	13.3±0.2	71 ±4	3.1 ±0.1	297 ±2	2.6±0.0
ROV 2	Starboard reactor	362±2	35.5±0.4	13.3±0.1	60 ±4	3.2 ±0.1	231 ±5	3.6±0.1
ROV 3	Stern	351±4	34.9±0.8	12.2±0.1	56 ±2	2.9 ±0.1	146 ±0	2.7±0.0
ROV 4	Port reactor	350±7	33.9±0.5	12.6±0.2	66 ±3	2.9 ±0.0	305 ±5	2.1±0.0

a - Norwegian data.
b - Dissolved by HNO_3.
For each case (n=3). Where SD is given as 0 and 0.0 SD was less than 5 and 0.5, respectively. Uncertainties on individual measurements were typically between 2% and 5%.

4.5 Radionuclides and trace elements in biota

4.5.1 Cs-137

The activity concentrations of Cs-137 in all pooled samples of the three fish species, cod (*Gadus morhua*), haddock (*Melanogrammus aeglefinus*) and common dab (*Limanda limanda*), were low (Table 4.16). These values were comparable to those observed in cod (*Gadus morhua*) sampled during the JNREG expedition in 2012 from the Pechora Sea (JNREG, 2014) and for various fish species samples from the Norwegian Sea and Barents Sea in 2014 (Skjerdal et al., 2017).

Table 4.16. Cs-137 activity concentrations (Bq/kg f.w.) in different fish species from the sampling area.

Species	Common name	Tissue	n	Cs-137[a] (Bq/kg f.w.)
Gadus morhua	Cod	Muscle	10	0.12 ±0.05
Melanogrammus aeglefinus	Haddock	Muscle	25	0.05 ±0.04
Limanda limanda	Common dab	Muscle	20	0.06 ±0.04

a - Norwegian data.
n - number of individual fish in pooled sample.

4.5.1 Trace elements

The concentrations of trace elements were determined in muscle, liver, kidney and gills of the three different fish species (Table 4.17). Fish were sampled from Station 20, a site shallower than the depth at which K-159 lies.

In general, there was a greater degree of variability in concentrations of trace elements between the different tissues for each species, than between the same tissues from the different fish species. Mean concentrations of Mn, Ni, Zn, Sr and U were generally highest in gills and higher in kidney than in liver and muscle. The concentration of Cd was highest in liver and the concentration of Cs was highest in muscle per dry weight tissue. The variation shown for Sr in muscle may indicate the presence of some bone material in these samples.

Table 4.17. Mean (±SD) concentration of selected trace elements (µg/g f.w.) in tissues of different fish species from the sampling area.

Trace element[a] (µg/g f.w.)	Tissue	Cod	Haddock	Common dab
Mn	Muscle	1.5 ±2.1	13 ±38	1.0 ±0.6
	Liver	2.1 ±0.4	2.1 ±0.4	-
	Kidney	1.7 ±0.5	1.6 ±0.0	4.6 ±2.1
	Gills	8 ±2	17 ±8	13 ±6
Fe	Muscle	65 ±92	39 ±68	40 ±61
	Liver	42 ±10	78 ±44	-
	Kidney	260 ±59	289 ±135	426 ±132
	Gills	141 ±43	222 ±120	294 ±394
Co	Muscle	0.05 ±0.12	0.02 ±0.01	0.03 ±0.01
	Liver	0.06 ±0.02	0.04 ±0.04	-
	Kidney	0.07 ±0.03	0.08 ±0.02	0.29 ±0.13
	Gills	0.04 ±0.02	0.07 ±0.05	0.09 ±0.08
Ni	Muscle	0.22 ±0.57	0.08 ±0.08	0.16 ±0.10
	Liver	0.06 ±0.02	0.22 ±0.09	-
	Kidney	0.20 ±0.10	0.35 ±0.08	2.4 ±1.6
	Gills	0.14 ±0.05	0.34 ±0.18	0.53 ±0.48
Zn	Muscle	25 ±6	23 ±6	23 ±4
	Liver	39 ±3	40 ±7	-
	Kidney	87 ±7	80 ±4	104 ±11
	Gills	72 ±26	86 ±7	109 ±44
Sr	Muscle	7 ±10	23 ±25	10 ±8
	Liver	1.1 ±0.7	1.9 ±2.2	-
	Kidney	3.9 ±4.1	0.7 ±0.1	0.5 ±0.2
	Gills	284 ±111	292 ±68	232 ±43
Cd	Muscle	0.01 ±0.01	0.01 ±0.00	0.01 ±0.01
	Liver	0.28 ±0.12	0.24 ±0.06	-
	Kidney	0.06 ±0.03	0.12 ±0.04	1.75 ±2.68
	Gills	0.04 ±0.01	0.13 ±0.22	0.05 ±0.02
Cs	Muscle	0.21 ±0.04	0.17 ±0.03	0.19 ±0.04
	Liver	0.02 ±0.00	0.01 ±0.00	-
	Kidney	0.09 ±0.01	0.06 ±0.01	0.04 ±0.01
	Gills	0.05 ±0.01	0.03 ±0.01	0.20 ±0.13
Pb	Muscle	0.10 ±0.07	0.08 ±0.09	0.07 ±0.05
	Liver	0.02 ±0.01	0.07 ±0.11	-
	Kidney	0.08 ±0.09	0.25 ±0.21	0.23 ±0.11
	Gills	0.15 ±0.07	0.51 ±0.69	0.33 ±0.44
U	Muscle	0.001 ±0.001	0.008 ±0.012	0.002 ±0.001
	Liver	0.001 ±0.001	0.002 ±0.002	-
	Kidney	0.001 ±0.002	0.003 ±0.003	0.023 ±0.010
	Gills	0.021 ±0.009	0.067 ±0.028	0.043 ±0.015

a - Norwegian data.

For each fish species, sample numbers (n) for each tissue (muscle, liver, kidney and gills) were as follows; Cod (10, 8, 6 and 10); Haddock (11, 8, 3 and 11); Common dab (10, 0, 10 and 10). Where SD is given as 0.00 SD was less than 0.05. Uncertainties on individual measurements were typically between 2% and 5%.

Trace element concentrations were determined in brittle stars and polychaete worms that were recovered from sediment samples taken at different sampling stations (Table 4.18). Trace element concentrations in individual specimens of the two different benthic fauna types varied considerably, but were higher in all cases than values for tissues of the 3 fish species sampled. Mean concentrations of trace elements in polychaete worms were higher than in brittle stars, with the exception of Zn, Sr and Cd.

Table 4.18. Mean (±SD) concentration of selected trace elements (µg/g f.w.) in brittle stars and polychaete worms from the sampling area.

Trace element[a] (µg/g f.w.)	Brittle stars (n=4)	Polychaete worms (n=4)
Mn	21 ±8	117 ±220
Fe	1308 ±493	9280 ±17443
Co	1.5 ±1.6	4.0 ±6.7
Ni	4.3 ±2.1	15 ±22
Zn	106 ±122	87 ±86
Sr	1117 ±822	320 ±326
Cd	4.1 ±6.4	0.55 ±0.67
Cs	0.44 ±0.28	0.69 ±1.14
Pb	1.6 ±0.8	4.4 ±7.0
U	0.35 ±0.03	1.2 ±2.0

a - Norwegian data.
Uncertainties on individual measurements were typically between 2% and 5%.

4.6 Derived parameters

4.6.1 Sediment distribution coefficients (K_d)

Sediment distribution coefficients (K_d) can be a useful indicator of the potential mobility of radionuclides from contaminated sediments. Radionuclides from a particular source may be present in the environment in different physico-chemical forms (e.g. low molecular mass species (LMM), colloids, particles) that can influence their bioavailability and ultimately determine the degree of doses, toxicity and effects that might be incurred by organisms. LMM species and colloids are generally considered to be mobile forms, while particles are more readily retained in sediments. If mobile species of radionuclides are present (low K_d values), transfer within an ecosystem will be a relatively rapid. If particles are present, (high K_d values), transfer within the ecosystem can be delayed or inhibited. In addition, the physico-chemical form of radionuclides deposited in the environment can change with time due to chemical interactions in the environment or to particle weathering.

K_d values for Cs-137 and Pu-239,240 in surface sediments from the sampling area (Table 4.19) were in general of the order of 1×10^3 and 1×10^5 respectively. This compares with previously reported K_d values of 7300 for Cs-137 and 8640 for Pu-239,240 for sediments further within Kola Bay (Brown et al., 2002). The K_d values observed for Cs-137 and Pu-239,240 in this study show good agreement with

recommended values (IAEA, 2004). The K_d value for I-129 for Station K-159 was 1.5 x 10^3 which was an order of magnitude higher than the recommended open ocean value for I (IAEA, 2004). Differences in K_d values may reflect differences in sediment type and grain size, salinities and/or the physico-chemical forms present.

K_d values for stable Sr and Cs were 7.7 and 1.2 x 10^4, respectively, which is the same order of magnitude as reported in coastal water from Japan (Uchida and Tagami, 2017). Thus, the K_d of stable Cs was one order of magnitude higher than the K_d for Cs-137, indicating a lower exchangeable fraction of stable Cs than for Cs-137. For other trace elements (Table 4.20), the derived K_d values for Mn, Fe, Co and U showed some variation to recommended values for these elements (IAEA, 2004). In particular, derived K_ds for Mn and Fe were orders of magnitude lower than recommended values for open oceans and ocean margins reflecting the influence of terrestrial sources of these elements to the area.

Table 4.19. Derived sediment distribution coefficients (K_d) for radionuclides in the sampling area.

	Cs-137	Pu-239,240	I-129
K-159	1.8E+03	9.1E+04	1.5E+03
Station 8	2.4E+03	4.6E+05	-
Station 12	2.6E+03	2.5E+05	-
Station 14	8.2E+02	1.5E+05	-
Station 18	2.3E+03	2.8E+05	-

K_d values based on activity concentration or concentration data from filtered bottom seawater (<1 µm for Cs-137 and <0.45 µm for Pu-239,240 and I-129) and from surface sediments collected at each sampling station (0-2 cm for Cs-137 and Pu-239,240 and mean value from sediments collected by ROV at locations close to the outer hull of K-159.for I-129).

Table 4.20. Derived sediment distribution coefficients (K_d) for trace elements at Station K-159.

	Mn	Fe	Co	Sr	Cs	U
K-159	9.3E+05	2.5E+04	1.1E+06	7.7E+00	1.2E+04	7.2E+02

K_d values derived using trace element concentration data from filtered bottom seawater (<0.45 µm) at Station K-159 and mean values from sediments collected by ROV at locations close to the outer hull of K-159.

4.6.2 Bioconcentration factors (BCF)

Bioconcentration factors (BCF) can vary according to the chemical species, the biological species and different internal organs and tissues. The speciation of radionuclides can affect their biological uptake, accumulation and biomagnification. For example, LMM-species can cross biological membranes, directly or indirectly after interactions with ligands or carrier molecules. Uptake in fish and invertebrates is commonly dependent on ionic species interacting with external organs (e.g. gills and skin) or through the digestion of food. In the case of filter feeding organisms, particles and colloids can be retained which may then undergo changes in bioavailability in the gut or be taken up by phagocytosis. BCF values derived for Cs-137 and trace elements in this study were based on seawater

samples taken from different stations than where fish samples were caught, so a degree of caution should be shown with regard to their interpretation.

The BCF values derived for Cs-137 in muscle for the three fish species were similar and of the order of 1×10^1 (Table 4.21), which was in good agreement with the recommended value of 50 for Cs in fish (IAEA, 2004). The BCF values derived for stable Cs in muscle were also similar between fish species (Table 4.22), but were an order of magnitude higher than for Cs-137.

For other trace elements in fish (Table 4.22), the derived BCFs for muscle for the 3 different fish species were in good agreement with recommend values (IAEA, 2004), with the exception of Cd where derived BCFs were an order of magnitude higher. BCFs for all elements for other tissues were generally similar to BCFs for muscle except for Mn (gills), Fe (kidney and gills), Sr (gills), Cd (liver, kidney and gills) and Ni (kidney and gills) where BCFs were at least one order of magnitude higher than for muscle. For trace elements in brittle stars and polychaete worms (Table 4.23), the derived whole body BCFs for all elements were one to two orders of magnitude higher than BCFs for muscle for the 3 fish species sampled.

Table 4.21. Derived biological concentration factors (BCF) for Cs-137 for fish species sampled.

Species	Common name	Tissue	Cs-137 (BCF)
Gadus morhua	Cod	Muscle	73
Melanogrammus aeglefinus	Haddock	Muscle	30
Limanda limanda	Common dab	Muscle	37

BCFs derived using the mean Cs-137 activity concentration of all filtered (<1 µm) bottom seawater samples and Cs-137 activity concentration data (f.w.) for each pooled fish sample.

Table 4.22. Derived biological concentration factors (BCF) for selected trace elements for different tissues of the fish species sampled.

Trace element	Tissue	Cod	Haddock	Common dab
Mn	Muscle	3.8E+03	3.2E+04	2.4E+03
	Liver	5.2E+03	5.2E+03	-
	Kidney	4.2E+03	3.9E+03	1.1E+04
	Gills	2.0E+04	4.3E+04	3.3E+04
Fe	Muscle	4.7E+04	2.9E+04	2.9E+04
	Liver	3.1E+04	5.7E+04	-
	Kidney	1.9E+05	2.1E+05	3.1E+05
	Gills	1.0E+05	1.6E+05	2.2E+05
Co	Muscle	1.1E+03	4.0E+02	5.4E+02
	Liver	1.2E+03	8.5E+02	-
	Kidney	1.5E+03	1.6E+03	6.1E+03
	Gills	7.9E+02	1.6E+03	2.0E+03
Ni	Muscle	9.9E+02	3.7E+02	6.9E+02
	Liver	2.6E+02	9.8E+02	-
	Kidney	8.9E+02	1.6E+03	1.1E+04
	Gills	6.3E+02	1.5E+03	2.3E+03
Sr	Muscle	9.3E-01	3.0E+00	1.4E+00
	Liver	1.5E-01	2.6E-01	-
	Kidney	5.2E-01	9.8E-02	6.6E-02
	Gills	3.8E+01	3.9E+01	3.1E+01
Cs	Muscle	8.1E+02	6.3E+02	7.3E+02
	Liver	6.4E+01	4.3E+01	-
	Kidney	3.4E+02	2.4E+02	1.5E+02
	Gills	1.8E+02	1.3E+02	7.8E+02
Cd	Muscle	6.4E+02	4.9E+02	6.9E+02
	Liver	1.9E+04	1.6E+04	-
	Kidney	3.8E+03	7.9E+03	1.2E+05
	Gills	2.6E+03	8.6E+03	3.5E+03
Pb	Muscle	1.4E+02	1.2E+02	9.9E+01
	Liver	3.0E+01	1.0E+02	-
	Kidney	1.2E+02	3.8E+02	3.5E+02
	Gills	2.3E+02	7.7E+02	5.0E+02
U	Muscle	4.9E-01	2.7E+00	6.2E-01
	Liver	3.6E-01	7.3E-01	-
	Kidney	4.5E-01	9.3E-01	7.7E+00
	Gills	7.1E+00	2.2E+01	1.4E+01

BCFs derived using the mean trace element concentration of all filtered (<0.45 µm) bottom seawater samples and the mean trace element concentration data (f.w.) for each tissue for each fish species.

Table 4.23. Derived biological concentration factors (BCF) for selected trace elements for brittle stars and polychaete worms sampled.

Trace element	Brittle stars	Polychaete worms
Mn	4.0E+04	2.9E+05
Fe	7.2E+05	6.8E+06
Co	2.4E+04	8.4E+04
Ni	1.9E+04	6.4E+04
Sr	1.1E+02	4.3E+01
Cs	1.7E+03	2.6E+03
Cd	2.1E+05	3.7E+04
Pb	2.5E+03	6.6E+03
U	8.9E+01	4.0E+02

BCFs derived using the mean trace element concentration of all filtered (<0.45 µm) bottom seawater samples and the mean trace element concentration data (f.w.) for each biota type.

5. Overall conclusions

The joint Norwegian-Russian cruise to investigate the radioecological status of the site of the sunken nuclear submarine K-159 in the Barents Sea was organized through the Norwegian-Russian expert group as one aspect of the greater cooperation between Norway and Russia with regard to nuclear safety and radiological environmental assessments. The joint Norwegian-Russian cruise in 2014 followed on from previous joint Norwegian-Russian cruises to dumping sites of radioactive waste in the Kara Sea and Novaya Zemlya fjords in the 1990s and in 2012.

In 2014, the nuclear submarine K-159 was observed lying upright at a depth of around 246 m at the entrance to Kola Bay. The inspection of the outer hull showed that a number of hatches are missing, that damage has occurred to areas of the deck and that there is a break in the hull towards the stern of the submarine. By comparison with photos of K-159 as it was being towed out from Gremikha in 2003, it is clear that the loss of the hatches and the observed damage to the deck and stern of the submarine must have occurred when or since K-159 sank.

Based on the in situ gamma measurements taken next to the submarine, the observed activity concentrations, activity ratios and atomic ratios in seawater and in sediment samples taken close to and in the area around the submarine, there is no indication of any leakage from the reactor units of K-159 to the marine environment.

Comparison of activity concentrations of Cs-137 in seawater and sediment samples with other marine areas from a similar time period suggests that the main source of Cs-137 to the area around K-159 is from the long-range ocean transport of Cs-137 from sources further afield. Activity concentrations of Cs-137 in fish from the sampling area were comparable to reported values for the Norwegian Sea and Barents Sea. Atomic ratios of Pu isotopes (Pu-240/Pu-239) in seawater and sediment samples indicated global fallout as the main source of these radionuclides. It is clear that there is a need for further work to identify the reasons behind the disparity in analytical results reported by Norway and Russia for Sr-90 in seawater.

Although there is currently no indication of any leakage from the reactor units of K-159 to the marine environment, further monitoring of the situation and status of the submarine is warranted. It is clear that K-159 has suffered further damage to its outer hull when or since it sank in 2003, including a break in the outer hull close to the stern. It was not possible during the joint Norwegian-Russian cruise in 2014 to determine whether the sinking and impact on the seafloor has had any effect on the inner pressure hull of K-159. Monitoring of the marine environment around K-159 should be followed closely, especially in connection with any future plans for the recovery of the submarine.

References

Aldahan, A., Englund, E., Possnert, G., Cato, I., Hou, X.L. 2007. Iodine-129 enrichment in sediment of the Baltic Sea. Applied Geochemistry 22(3): 637-647.

AMAP. 2016. AMAP Assessment 2015: Radioactivity in the Arctic. Arctic Monitoring and Assessment Programme (AMAP), Oslo, Norway.

BfS/BMU. 2014. Umweltradioaktivität und Strahlenbelastung: Jahresbericht 2012. Bundesamt für Strahlenschutz (BfS) und Bundesministerium für Umwelt, Naturschutz und Reaktorsicherheit (BMU).

BfS/BMU. 2017. Umweltradioaktivität und Strahlenbelastung: Jahresbericht 2014 Bundesamt für Strahlenschutz (BfS) und Bundesministerium für Umwelt, Naturschutz und Reaktorsicherheit (BMU). In prep.

Brown, J.E., Nikitin, A., Valetova, N.K., Chumichev, V.B., Katrich, I.Y., Berezhnoy, V.I., Pegoev, N.N., Kabanov, A.I., Pichugin, S.N., Vopiyashin, Y.Y., Lind, B. 2002. Radioactive contamination in the marine environment adjacent to the outfall of the radioactive waste treatment plant at ATOMFLOT, northern Russia. Journal of Environmental Radioactivity 61(1): 111-131.

Calvo, E.C., Santos, F.J., Lopez-Gutierrez, J.M., Padilla, S., Garcia-Leon, M., Heinemeier, J., Schnabel, C., Scognamiglio, G., 2015. Status report of the 1 MV AMS facility at the Centro Nacional de Aceleradores. Nuclear Instruments & Methods in Physics Research Section B-Beam Interactions with Materials and Atoms 361, 13-19.

Chamizo, E., Jimenez-Ramos, M.C., Wacker, L., Vioque, I., Calleja, A., Garcia-Leon, M., Garcia-Tenorio, R. 2008a. Isolation of Pu-isotopes from environmental samples using ion chromatography for accelerator mass spectrometry and alpha spectrometry. Analytica Chimica Acta 606: 239-245.

Chamizo, E., Lopez-Gutierrez, J.M., Ruiz-Gomez, A., Santos, F.J., Garcia-Leon, M., Maden, C., Alfimov, V. 2008b. Status of the compact 1 MV AMS facility at the Centro Nacional de Aceleradores (Spain). Nuclear Instruments & Methods in Physics Research Section B-Beam Interactions with Materials and Atoms 266: 2217-2220.

EPA. 2016. Draft Radioactivity in Seawater 2014-2015. Environmental Protection Agency of Ireland.

Gómez-Guzmán, J.M., López-Gutiérrez, J.M., Pinto-Gómez, A.R., Holm, E. 2012. ^{129}I measurements on the 1 MV AMS facility at the Centro Nacional de Aceleradores (CNA, Spain). Applied Radiation and Isotopes 70: 263-268.

Guidelines, 1986. Methodological guidelines on determination of radioactive contamination of water bodies.- Edited by S.M.Vakulovsky. - Moscow, Hydrometeoizdat (in Russian).

Hardy, E.P., Krey, P.W., Volchock, H.L. 1973. Global inventory and distribution of fallout plutonium. Nature 24: 444–445.

HELCOM. 2015. HELCOM MORS Environmental Database. HELCOM – Baltic Marine Environment Protection Commission, Helsinki.

Hou, X.L., Fogh, C.L., Kucera, J., Andersson, K.G., Dahlgaard, H. and Nielsen, S.P. 2003. Iodine-129 and Caesium-137 in Chernobyl contaminated soil and their chemical fractionation. Science of the Total Environment 308(1): 97-109.

Hou, X., Hansen, V., Aldahan, A., Possnert, G., Lind, O.C., Lujaniene, G. 2009. A review on speciation of iodine-129 in the environmental and biological samples. Analytica Chimica Acta 632: 181-196.

IAEA. 1989. Measurements of Radionuclides in the Environment. A Guidebook. Technical Report Series No. 295. IAEA, Vienna.

IAEA. 1999. Inventory of radioactive waste disposal at sea. IAEA-TECDOC-1105, IAEA, Vienna.

IAEA. 2004. Sediment distribution coefficients and concentration factors for biota in the marine environment. Technical Reports Series No. 422. IAEA, Vienna.

IAEA. 2015. Inventory of Radioactive Material Resulting from Historical Dumping, Accidents and Losses at Sea. 2015. IAEA-TECDOC-1776, IAEA, Vienna.

JNREG. 1996. Dumping of radioactive waste and radioactive contamination in the Kara Sea. Results from 3 years of investigations (1992-1994) by the Joint Norwegian Russian Expert Group. Norwegian Radiation Protection Authority, Østerås.

JNREG. 2014. Joint Norwegian-Russian Expert Group investigation into the radioecological status of Stepovogo Fjord: The dumping site of the nuclear submarine K-27 and solid radioactive waste. Results from the 2012 research cruise performed by the Joint Norwegian-Russian Expert Group.- Edited by Justin P. Gwynn and Alexander I. Nikitin.- Joint Norwegian-Russian Expert Group for investigation of Radioactive Contamination in the Northern Areas, 2014.

Kazennov, A. 2010. Technologies of radiation monitoring of dumped objects and aquatories. The practices of RRC "Kurchatov Institute". Presentation at the IAEA CEG Workshop on Removal of Spent Nuclear Fuel (SNF) and Radioactive Waste (RW) from Andreeva Bay, and Strategies for Handling Sunken Objects Containing SNF in the Arctic Ocean. 24 - 26 February 2010, Hague, Netherlands. https://www.iaea.org/OurWork/ST/NE/NEFW/CEG/documents/ws022010/eng/5.4KazennovEngl.pdf

Kelley, J.M., Bond, L.A., Beasley, T.M. 1999. Global distribution of Pu isotopes and 237Np. Science of the Total Environment 237–238: 483-500.

Klein, M.G., Mous, D.J.W., Gottdang, A. 2006. A compact 1 MV multi-element AMS system. Nuclear Instruments & Methods in Physics Research Section B-Beam Interactions with Materials and Atoms 249: 764-767.

Klein, M.G., Van Staveren, H.J., Mous, D.J.W., Gottdang, A. 2007. Performance of the compact HVE 1 MV multi-element AMS system. Nuclear Instruments & Methods in Physics Research Section B-Beam Interactions with Materials and Atoms 259: 184-187.

Leppänen, A.P., Kasatkina, N., Vaaramaa, K., Matishov, G.G., Solatie, D. 2013. Selected anthropogenic and natural radioisotopes in the Barents Sea and off the western coast of Svalbard. Journal of Environmental Radioactivity 126: 196-208.

Lopez-Gutierrez, J.M., Garcia-Leon, M., Schnabel, C., Suter, M., Synal, H.A., Szidat, S., Garcia-Tenorio, R. 2004. Relative influence of I-129 sources in a sediment core from the Kattegat area. Science of the Total Environment 323: 195-210.

López-Lora, M., Chamizo, E., Villa-Alfageme, M., Hurtado-Bermúdez, S., Casacuberta, N., García-León, M. 2018. Isolation of ^{236}U and ^{239,240}Pu from seawater samples and its determination by Accelerator Mass Spectrometry. Talanta 178: 202-210.

Martin, P., Hancock, G.J. 2004. Routine analysis of naturally occurring radionuclides in environmental samples by alpha-particle spectrometry. Supervising Scientist Report 180, Supervising Scientist, Darwin NT.

Matishov, G.G., Matishov, D.G., Namjatov, A.A., Carroll, J. and Dahle, S. 1999. Anthropogenic radionuclides in Kola and Motovsky Bays of the Barents Sea, Russia. Journal of Environmental Radioactivity 43(1): 77-88.

Methods. 1995. Methods of monitoring radioactive contamination of water bodies (MVI.01.-7/96).- Edited by A.I.Nikitin.- Obninsk, RPA "Typhoon" (in Russian).

MMBI/ApN. 2015. Present radioactivity levels in the physical environment and biota of Andreeva Bay (2015). Murmansk Marine Biological Institute and Akvaplan-niva AS.

Hosseini, A., Amundsen, I., Brown, J., Dowdall, M., Dyve, J.E., Klein, H. 2017. Environmental modelling and radiological impact assessment associated with hypothetical accident scenarios for the Russian nuclear submarine K-159. StrålevernRapport 2017:12. Norwegian Radiation Protection Authority, Østerås.

Oughton, D.H., Fifield, L.K., Day, J.P., Cresswell, R.C., Skipperud, L., Salbu, B. 1999. Determination of ^{240}Pu/^{239}Pu isotope ratios in Kara Sea and Novaya Zemlya sediments using accelerator mass spectrometry. In: Symposium on Marine Pollution, IAEA-SM-354, IAEA, Vienna.

Procedure. 2004. Procedure of determination of Pu-239,240 content in samples of environmental materials with radiochemical concentrating and using alpha spectrometer (MVI 45090. 4B004).- Obninsk, RPA "Typhoon", (in Russian).

Raisbeck, G.M., Yiou, F., Zhou, Z.Q., Kilius, L.R., Dahlgaard, H. 1993. Anthropogenic 129I in the Kara Sea, in: Holm, E. (Ed.), Environmental radioactivity in the Arctic and Antarctic. Proceedings. Norwegian Radiation Protection Authority, Østerås, pp. 125-128.

Rearden B.T., Jessee M.A. 2016. SCALE Code System, ORNL/TM-2005/39, Version 6.2.1. Oak Ridge, Tennessee: Oak Ridge National Laboratory, 2016.

RIFE. 2015. Radionuclides in food and the environment, 2014. RIFE-20, Cefas, UK.

Sarkisov, A.A., Sivintsev, Y.V., Vysotskiy, V.L., Nikitin V.S. 2009. Atomic legacy of the cold war at the Arctic seabed: Radioecological consequences and technical and economic problems of radiation remediation at the Arctic Seas. Moscow: Nuclear Safety Institute, 2009.

Sivintsev, Yu.V., Vakulovsky, S.M., Vasiliev, A.P., Vysotsky, V.L., Gubin, A.T., Danilyan, V.A., Kobzev, V.I., Kryshev, I.I., Lavkovsky, S.A., Mazokin, V.A., Nikitin, A.I., Petrov, O.I., Pologikh, B.G., Skorik, Yu.I. 2005.

Technogenic radionuclides in the sea surrounding Russia. Radioecological Consequences of Radioactive Waste Dumping in the Arctic and Far Eastern Seas 'The White Book – 2000', Moscow.

Skjerdal, H., Heldal, H.E., Gwynn, J., Strålberg, E., Liebig, P.L., Møller, B., Gäfvert, T., Rudjord, A.L. 2017. Radioactivity in the Marine Environment 2012, 2013 and 2014. Results from the Norwegian Marine Monitoring Programme (RAME). StrålevernRapport 2017:13. Norwegian Radiation Protection Authority, Østerås.

Smith, J.N., Ellis, K.M., Polyak, L., Ivanov, G., Forman, S.L., Moran, S.B. 2000. ^{239,240}Pu transport into the Arctic Ocean from underwater nuclear tests in Chernaya Fjord, Novaya Zemlya. Continental Shelf Research 20: 255-279.

Sneve, M.K., Kiselev, M., Shandala, N.K. 2014. Radioecological characterization and radiological assessment in support of regulatory supervision of legacy sites in northwest Russia. Journal of Environmental Radioactivity 131: 110-118.

Sutton, D.C., Kelly, J.J., 1968. Strontium-90 and cesium-137 measurements of large volume sea water samples. HASL-196, USAEC Report, New York.

UNSCEAR. 1993. Sources and Effects of Ionizing Radiation. United Nations Scientific Committee on the Effects of Atomic Radiation, United Nations, New York.

UNSCEAR. 2000. Sources and Effects of Ionizing Radiation. United Nations Scientific Committee on the Effects of Atomic Radiation, United Nations, New York.

Uchida, S., Tagami, K. 2017. Comparison of coastal area sediment-seawater distribution coefficients (K_d) of stable and radioactive Sr and Cs. Applied Geochemistry 85: 148-153.

Vasin, S.E., Kazennov, A., Korolev, A.V. 2011. Organization of international expedition for radiation monitoring of B-159. Presentation at the IAEA CEG Workshop on The Investigation of Nuclear Submarines and Objects with Spent Nuclear Fuel and Radioactive Wastes Sunken in the Arctic Seas and Strategies for Radio Ecological Rehabilitation of the Arctic Region, 16 - 17 February 2011, Oslo, Norway. https://www.iaea.org/OurWork/ST/NE/NEFW/CEG/documents/ws022011/eng/2.3_Korolev_Engl.pdf

Varskog, P., Bjerk, T.O., Ruud, A.B. 1997. pH-controlled EDTA titration as an alternative method for determination of the chemical yield of yttrium in ^{90}Sr-analysis, in: Proceedings of Rapid Radioactivity Measurements in Emergency and Routine Situations, The National Physical Laboratory, Teddington, pp. 237-241.

Wendel, C.C., Fifield, L.K., Oughton, D.H., Lind, O.C., Skipperud, L., Bartnicki, J., Tims, S.G., Høibråten, S., Salbu, B. 2013. Long-range tropospheric transport of uranium and plutonium weapons fallout from Semipalatinsk nuclear test site to Norway. Environment International 59: 92-102.

White Book. 1993. Facts and problems related to radioactive waste disposal in seas adjacent to the territory of the Russian Federation. Office of the President of the Russian Federation, Moscow.

Yiou, F., Raisbeck, G., Imbaud, H. 2004. Extraction and AMS measurement of carrier free I-129/I-127 from seawater. Nuclear Instruments & Methods in Physics Research Section B-Beam Interactions with Materials and Atoms 223, 412-415.